



HHS Public Access

Author manuscript

J Med Chem. Author manuscript; available in PMC 2020 January 28.

Published in final edited form as:

J Med Chem. 2020 January 23; 63(2): 656–675. doi:10.1021/acs.jmedchem.9b01608.

Discovery and Structure-Based Optimization of Potent and Selective WDR5 Inhibitors Containing a Dihydroisoquinolinone Bicyclic Core

Jianhua Tian⁶, Kevin B. Teuscher¹, Erin R. Aho², Joseph R. Alvarado¹, Jonathan J. Mills¹, Kenneth M. Meyers¹, Rocco D. Gogliotti¹, Changho Han¹, Jonathan D. Macdonald¹, Jiqing Sai¹, J. Grace Shaw¹, John L. Sensintaffar¹, Bin Zhao¹, Tyson A. Rietz¹, Lance R. Thomas², William G. Payne¹, William J. Moore⁷, Gordon M. Stott⁷, Jumpei Kondo^{8,9}, Masahiro Inoue^{8,9}, Robert J. Coffey^{2,4}, William P. Tansey², Shaun R. Stauffer¹, Taekyu Lee¹, Stephen W. Fesik^{1,3,5,*}

¹Department of Biochemistry, Vanderbilt University School of Medicine, Nashville, Tennessee 37232, USA

²Department of Cell and Developmental Biology, Vanderbilt University School of Medicine, Nashville, Tennessee 37232, USA

³Department of Pharmacology, Vanderbilt University School of Medicine, Nashville, Tennessee 37232, USA

⁴Department of Medicine, Vanderbilt University School of Medicine, Nashville, Tennessee 37232, USA

⁵Department of Chemistry, Vanderbilt University, Nashville, Tennessee 37232, USA

⁶Chemical Synthesis Core, Vanderbilt Institute of Chemical Biology, Vanderbilt University, Nashville, Tennessee 37232, USA

⁷Leidos Biomedical Research, Frederick National Laboratory for Cancer Research, Frederick, MD 21701, USA

⁸Department of Clinical Bio-resource Research and Development, Graduate School of Medicine, Kyoto University, Kyoto, 606-8501, Japan

⁹Department of Biochemistry, Osaka International Cancer Institute, Osaka, 541-8567, Japan

*Corresponding Author: Stephen.fesik@vanderbilt.edu. Phone: +1 (615) 322-6303. Fax: +1 (615) 875-3236.

Author Contributions

JT, KBT, JRA, JJM, KMM, RDG, CH, and JDM designed and synthesized compounds. ERA and LRT conducted mechanism of action studies featured in Figure 4,5 and 7. JS and JGS obtained the biochemical and cell-based data in Table 1–3. JLS conducted western blot and caspase assay in Figure 6. BZ, TAR, and WGP performed X-ray crystallography studies of complexes. JK, MI, and RJC conducted CTOSs assay in Figure 8. WJM GMS helped design experiments. WPT, SRS, TL, and SWF design and directed experiments and helped write the paper. All authors have given approval to the final version of the manuscript.

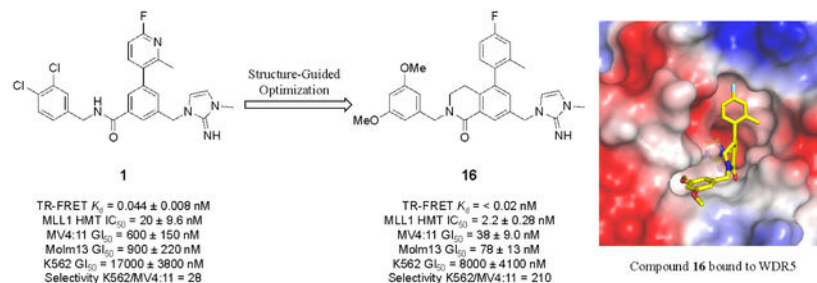
Supporting Information. X-ray refinement statistics, MLL1 HMT assay details and titration curves of compound **16**. This material is available free of charge via the internet at <http://pubs.acs.org>.

Accession Codes. Atom coordinates and structure factors for WDR5-ligand complexes can be accessed in the PDB via the following accession codes: Compound **13**/WDR5 complex (6UFX), Compound **16**/WDR5 complex (6UCS). Authors will release the atomic coordinates upon article publication.

Abstract

WD repeat domain 5 (WDR5) is a member of the WD40-repeat protein family that plays a critical role in multiple chromatin-centric processes. Overexpression of WDR5 correlates with poor clinical outcome in many human cancers, and WDR5 itself has emerged as an attractive target for therapy. Most drug-discovery efforts center on the WIN site of WDR5 that is responsible for recruitment of WDR5 to chromatin. Here, we describe discovery of a novel WDR5 WIN site antagonists containing a dihydroisoquinolinone bicyclic core using structure-based design. These compounds exhibit picomolar binding affinity and selective concentration-dependent anti-proliferative activities in sensitive MLL-fusion cell lines. Furthermore, these WDR5 WIN site binders inhibit proliferation in MYC-driven cancer cells and reduce MYC recruitment to chromatin at MYC/WDR5 co-bound genes. Thus, these molecules are useful probes to study the implication of WDR5 inhibition in cancers and serve as a potential starting point toward the discovery of anti-WDR5 therapeutics.

Graphical Abstract



Keywords

WDR5; WIN site inhibitor; structure-based design; mixed-lineage leukemia

INTRODUCTION

WD repeat domain 5 (WDR5) is a member of the WD40-repeat protein family^{1–3} and functions as a core scaffolding component in multiple protein complexes that control transcriptional regulation and histone code modification processes as a part of the epigenetic machinery.⁴ WDR5 maintains over 90% sequence homology among all vertebrates to form a characteristic circular barrel shaped 7-bladed β -propeller structure and provides two major interfaces, where a number of partner proteins can bind. The most prominent role of WDR5 is in the context of MLL/SET complexes that deposit histone H3 lysine 4 di- and trimethylation (H3K4me2, me3),^{5–8} a mark of transcriptionally active chromatin. Binding interactions between WDR5 and members of the MLL/SET family of proteins (MLL1–4, SETd1A, and SETd1B) are well-characterized,^{9–12} and center on interaction of a conserved arginine in the MLL/SET proteins with an arginine-binding cavity on WDR5 known as the WIN site. In these complexes, WDR5 also interacts with at least three other proteins (RBBP5, ASH2L, and DPY30) through WIN-site independent mechanisms. Although all

MLL/SET family members can engage the WIN site, complexes containing MLL1 are uniquely dependent on the WIN site of WDR5 for enzymatic activity.¹³

WDR5 is also involved in the association of MYC oncoprotein transcription factors with chromatin¹⁴. MYC does not bind WDR5 via the WIN site, but instead interacts with a distal cleft (the WBM site) that is also bound by RBBP5. WDR5 co-localizes with MYC on chromatin at key target genes, and mutations in MYC that disrupt the interaction with WDR5 reduce the binding of MYC to chromatin, and disable its pro-tumorigenic properties *in vivo*. WDR5 thus serves as a critical co-factor for MYC proteins to execute malignant gene expression programs. Furthermore, several cancers exhibit aberrant overexpression of WDR5 including bladder cancer,¹⁵ pancreatic cancer,¹⁶ breast cancer,⁵ colorectal cancer,¹⁷ gastric cancer,¹⁸ prostate cancer,^{19,20} neuroblastoma,²¹ head neck squamous cell carcinoma,²² and various leukemias.²³ Often, overexpression of WDR5 is found in more aggressive cancers, and is associated with poor prognoses.^{15,17,24} Considering the multifaceted role of WDR5 in human malignancies, WDR5 has emerged as an attractive drug target for discovery of potent small molecule inhibitors.

Most drug discovery efforts targeting WDR5 center on the WIN site. The concept of targeting the WIN site of WDR5 as a therapeutic strategy first arose within the context of leukemias characterized by translocations of the MLL1 gene.^{11,25,26} In these cancers, translocation of a single allele in the 11q23 *MLL1* gene to one of more than 70 different partner genes results in the development of leukemia.^{11,25,26} The most common fusion partners AF4, AF9, and ENL account for 70% of acute lymphoid leukemia (ALL) in infants and 5–10% of acute myeloid leukemia (AML) in adults.^{26–28} It was originally proposed²⁹ that MLL-rearranged cancers would be sensitive to WIN site inhibitors because of a dependency on the remaining pristine MLL1 allele in these cancers, but this rationale has since been disproved.³⁰ There is, however, a strong empirical sensitivity of MLL-fusion cancer cells to WIN site inhibitors,³¹ supporting the idea that they can be implemented for treatment of these malignancies.

Several structurally distinctive classes of WDR5 WIN site inhibitors have been reported, and Figure 1 depicts three representative classes of which their binding interactions at the site have been confirmed by X-ray co-crystal structures. Macrocyclic peptidomimetic compounds were designed to mimic the MLL peptide residues within the WIN site. MM-589 (Figure 1)³² was reported to exhibit sub-nanomolar affinity at the WIN site, selective inhibition of MLL1 HMT activity with low-nanomolar IC₅₀, and anti-proliferative activities in MLL-fusion cancer cell lines MV4:11 and Molm13. OICR-9429 (Figure 1)^{33,34} is an example of non-peptidomimetic small-molecule WIN site inhibitor, wherein a basic methyl-piperazine moiety mimics the guanidine side-chain of R3765 in the MLL peptide. This compound has a reported K_i of 64 nM to WDR5 and has demonstrated reduced viability of primary human AML cells that express mutant forms of CCAAT-enhancer-binding protein α (C/EBP α)³³ and gain-of-function p53 mutants.⁶

We have previously reported the discovery of WDR5 inhibitors using fragment-based methods and structure-based design.^{8,35} Our second-generation chemical probe was discovered using the imidazole-imine “warhead” moiety, which mimics the R3765 side-

chain in the S₂ pocket. The key binding interaction elements, such as a sandwiched π - π stacking interaction of the imidazole-imine in the S₂ pocket, hydrogen-bond interaction of the carbonyl oxygen with the backbone NH of C261, and a hydrophobic biaryl moiety within the S₄ pocket, mediated favorable binding of **1** (Figure 1)⁸ with a K_i of 44 pM to WDR5. Compound **1** also inhibited MLL1 HMT with low-nanomolar activity and proliferation of MLL-fusion cell lines MV4:11 and Molm13 with a GI₅₀ values of 600 and 900 nM, respectively in a five-day cell proliferation assay. Compound **1** was then used as a chemical probe to investigate the implication of WDR5 WIN site inhibition on the interaction of WDR5 with chromatin, transcriptional alterations, and cellular functions that impact cell-fate. We found that blocking the WIN site of WDR5 with compound **1** caused displacement of WDR5 protein from its binding sites on chromatin and triggered a series of events including decreased expression of WDR5-bound ribosome protein genes, induction of nucleolar stress, increased p53 translation, and activation of p53-dependent apoptosis. Our previous results forecast a broad utility of potent WDR5 inhibitors as potential therapeutics against cancers.

Despite the picomolar binding affinity of compound **1**, further improvements in cellular potency and pharmaceutical properties need to be made in order to demonstrate the therapeutic potential of WDR5 inhibitors. Here, we report our continued efforts to develop a potent and selective WDR5 inhibitor that builds upon our recently reported compound **1**. Our efforts led to the discovery of a new class of potent WDR5 inhibitors that contain a novel dihydroisoquinolinone core unit, which was designed using X-ray structure-guided modifications. The new series of inhibitors offer significantly enhanced on-target mechanism-based anti-proliferative activity in WDR5 sensitive cells and drug-like properties. These improved compounds also produce consistent biomarker changes at physiologically relevant concentrations which support the primary mechanism of action.⁸

RESULTS AND DISCUSSION

Optimization of the Substituted Benzamide Series WDR5 Inhibitors Using Pharmacophore-based Approach.

The structure of compound **1** was divided into four pharmacophore units (P₂, P₄, P₇, and core) based on their binding sub-site alignments in the WIN site of WDR5 with residues 3764–3773 (ARAEVHLRKS) in MLL1,³⁶ and focused SAR efforts on each sub-unit were performed to optimize the potency and pharmaceutical properties of the series. The biochemical activity of each inhibitor was profiled using a time-resolved fluorescence energy transfer (TR-FRET) assay to determine the competitive binding affinity (K_i) against the MLL1 derived FITC-peptide probe followed by a H3K4 HMT inhibition assay as an orthogonal functional measurement of the effect on MLL1 mediated HMT activity.

As previously reported,⁸ WDR5 WIN site inhibitors display a robust antiproliferative response in MLL-fusion cancer cell lines that express wild-type p53. Therefore, WDR5 inhibition mediated cellular efficacy was assessed in MV4:11 and Molm13. The K562 leukemia cell line, which is null for p53, was used as an insensitive control. The half-maximal growth inhibition (GI₅₀) ratio between K562 and MV4:11 serves as a cellular selectivity measure to ascertain primary target mediated activity.

The benzyl-3-methyl-1,3-dihydro-2*H*-imidazol-2-imine moiety of compound **1** bound to the deepest part of the WIN-site was incorporated into the new compound design for consistency in activity comparisons. The potentially reactive 4-fluoro-2-methylpyridin-3-yl P₄ moiety of **1** was replaced with the chemically more stable 4-fluoro-2-methylphenyl isostere. We then set out to optimize the P₇ moiety located in the hydrophobic S₇ pocket of the WIN-site where H3769 and L3770 of MLL1 bind. A focused library of substituted benzamides was constructed by employing more than 50 benzylamines with varying substitution patterns and sizes to probe binding interactions at the site. Table 1 depicts representative examples to illustrate SAR trends.

Compound **2** was designed to establish the baseline activity profile of the unsubstituted phenyl moiety, and exhibited low-nanomolar binding affinity ($K_i = 1.5$ nM) to WDR5, inhibition of HMT with IC₅₀ of 43 nM and low-micromolar anti-proliferative activity in the sensitive cell lines with only 5-fold selectivity over K562 cells. Early analogs indicated that the mono meta-substitution of phenyl group was more beneficial than other positions; therefore, a series of 3-substituted phenyl analogues were introduced to determine the optimal substituent in the S₇ pocket. Compound **3** with a 3-methylphenyl demonstrated a marginal improvement in binding affinity, which was not translated in cellular potency in the sensitive cell lines. However, compounds **4** and **5** bearing either a 3-chloro or 3-methoxy groups displayed an order of magnitude enhanced binding affinities with sub-micromolar GI₅₀'s in sensitive cell lines. In general, functional HMT IC₅₀ values show good correlation and rank order with the cellular anti-proliferative activities (GI₅₀) in the sensitive cell lines. For example **5** displayed a 4-fold improvement in HMT activity when compared to **2** and indeed **5** was consistently more potent in cells than **2**. Interestingly, the 3-trifluoromethoxy of compound **6** exerted an undesirable binding interaction at the site to cause a large decrease in binding affinity and cellular activity. From this subset of mono-substituted compounds, 3-chloro and 3-methoxy groups provided beneficial binding interactions in the S₇ pocket and were utilized in further optimization of the P₇ unit.

We next explored either 3,4- or 3,5-disubstituted phenyl analogues for improved potency targeting the S₇ sub-site in biochemical and cellular assays. Compound **7** containing 3,4-dichloro substitutions demonstrated a slight improvement in binding and cellular potency over its direct analog **1**. This result also confirmed that replacement of the P₄ group to the 4-fluoro-2-methylphenyl also proved to be beneficial to the *in vitro* potency of compounds. When compared to **4**, the additional 4-chloro group in **7** also increased both binding affinity and HMT inhibition by 4 to 5-fold, and resulted in 2-fold enhanced cellular activity in the sensitive cell lines. As seen previously, compound **8** with 3-methyl-4-chloro substitution exhibited 3-fold reduced biological activities compared to **7**, which is consistent with **3** and suggests that the 3-methyl group is a suboptimal phenyl substituent in the S₇ sub-pocket for WDR5 potency. The 4-fluoro group in **9** and **10** were beneficial and added potency to existing 3-substituents of the phenyl group. Indeed, compound **10** with 4-fluoro-3-methoxyphenyl P₇ moiety displayed the highest cellular potency in both MV4:11 and Molm-13 cells and selectivity over the insensitive K562 among examples in Table 1. The 3,5-disubstituted phenyl P₇ compounds, represented by **11** – **13**, were found to be equally effective by displaying similar *in vitro* potency compared to the 3,4-disubstituted series

compounds. In summary, the 3-substituent of the phenyl P₇ group is essential for the baseline affinity to the WIN site of WDR5, and the proper second substitutions at the 4- or 5-position are equally beneficial for enhancing potency further. Finally, compounds **5**, **10** and **13** with the 3-methoxy substitution exhibited significantly improved GI₅₀ ratios between MV4:11 and K562 compared to the 3-chloro or 3-methyl analogs. These results suggest that observed selective cytotoxicity in MV4:11 by the 3-methoxy series were mainly driven by the WDR5 inhibition mechanism, but they were generally less cytotoxic in insensitive cells. Based on the affinity, promising cellular activity, and selectivity index, compound **13** was chosen for further characterization and SAR expansion.

X-ray Co-crystal Structure of **13** Bound to WDR5.

An X-ray co-crystal structure of compound **13** bound to WDR5 (Figure 2) was obtained to determine the binding interactions at the WIN site for further structure-based design optimization. The binding mode of **13** bound to WDR5 (Figure 2A) was similar to the previously reported structure⁸ of **1**.

The imidazole imine P₂ group is positioned deeply in the S₂ sub-pocket to engage double π - π stacking interactions with F133 and F263 and H-bond interaction to the carbonyl oxygen of C261 residue of WDR5. In addition, the imine NH formed two H-bond interactions with the backbone carbonyl oxygen of C261 with an interatomic distance of 2.8 Å and water bridged interaction to the side chains of S175 and S218 residues. The 4-fluoro-2-methylphenyl and 3,5-dimethoxyphenyl occupy the hydrophobic S₄ and S₇ sub-sites, respectively. The 3-methoxy unit the P₇ group penetrates to the deepest part of S₇ pocket to have hydrophobic interactions. Conversely, the 5-methoxy moiety is positioned toward the solvent accessible area where further chemical modifications are feasible for incorporation of property optimizing groups. An additional H-bond is also identified between the carbonyl of the benzamide core and the backbone NH of C261 with an interatomic distance of 2.8 Å, which is essential to stabilize the exit vector to the P₇ group. The previously described key binding interaction elements of **13** (Figure 2B) contribute greatly to the overall binding affinity.

The X-ray structure of **13** revealed an opportunity for further structural modification of the core unit. Figure 2C highlights the bioactive conformation and positions on the core phenyl ring and the amide NH, where two hydrogen atoms provide appropriate vectors for a ring constraint design through a saturated bicyclic ring system to restrict the conformation. This modification may have several expected benefits. First, the new bicyclic core would preserve the binding conformation of the core unit and potentially increase the binding affinity by reducing conformational entropy. Second, the modification would effectively eliminate a potentially metabolically unstable secondary amide functional group, an H-bond donor, and two rotatable bonds that in principle may benefit pharmacokinetic and pharmaceutical properties of final target compounds.

Dihydroisoquinolinone Series WDR5 Inhibitors.

To further improve potency and pharmaceutical properties of the compounds, the tether design strategy was applied to form the dihydroisoquinoline core. Compounds **14** – **16**

(Table 2) bearing optimized P₇ units were synthesized, and they exhibited significantly enhanced biological activities compared to their direct open-chain analogs. Compound **14** had a 3 to 6-fold improvement in binding affinity, HMT inhibition and antiproliferative activity in the sensitive cell lines compared to **8**. Binding affinities and HMT activities for both **15** and **16** could not be measured reliably because their IC₅₀'s from our TR-FRET and HMT assays were below or at the theoretical limit of detection. The improved WDR5 affinities of **15** and **16** also impacted cellular potency of both compounds by lowering their GI₅₀'s 6- to 12-fold only in the sensitive cell lines compared to **9** and **13**. As expected, the cellular selectivity ratios assessed by GI₅₀ differences between K562 and MV4:11 lines were significantly increased to 120 and 210 for **15** and **16**, respectively. The results indicate that the structural modification on the core unit enhances the WDR5 affinity, which is translated to an increase in on-target mediated anti-proliferative activity in the WDR5 sensitive cells.

Compound **17** – **22** (Table 2) bearing P₂ variations on the compound **16** scaffold were synthesized and evaluated for their biological activities. P₂ variants were selected on the basis of X-ray co-crystal structure of **16** bound to WDR5 (Figure 3) in which all beneficial interactions of the methyl imidazole imine moiety in the S₂ pocket were preserved. The increased size and hydrophobicity of the P₂ group using cyclopropyl in **17** and **18** caused the reduction in cellular potency in sensitive lines despite potent binding affinities and HMT inhibition activities. Compound **19** – **22** containing bioisosteres of the imidazole imine P₂ group also exhibited reduced cellular potency in MV4:11 and Molm-13 cells compared to compound **16**. Furthermore, **20** and **21** showed significantly diminished cellular selectivity, which may suggest an increase in cytotoxicity by off-target mechanisms. These results indicate the P₂ moiety is a crucial component for cellular potency and selectivity. Finally, **16** with the methyl imidazole imine exhibited the best overall profile and was chosen as a chemical probe to interrogate the biological consequence of WDR5 inhibition.

X-ray Co-crystal Structure of **16** Bound to WDR5.

To confirm the binding mode of the dihydroisoquinolinone core unit, the X-ray co-crystal structure of compound **16** bound to WDR5 (Figure 3) was obtained. The side view of the X-ray structure (Figure 3A) displays the same key binding interactions, such as the sandwich π – π stacking with side chain residues F133 and F263, bidentate H-bond with C261, and water mediated H-bond with side chain residues S175 and S218, as reported for **13** (Figure 2B). Overlays of the WDR5 bound conformations of **13** (green, Figure 3B) and **16** (yellow, Figure 3B) are nearly superimposable to further support the structure-based design. The ethylene tether of the dihydroisoquinolinone core is positioned in an unoccupied area of the WIN site and has no significant direct interactions within this region of the WIN-site. Therefore, the observed potency enhancement of compound **16** may be mainly mediated by reducing the conformational entropy by fixing the benzamide core conformation and the exit vector to the S₇ sub-pocket.

Evidence of target engagement in cells.

We were interested in investigating whether inhibitor **16** is able to engage the WIN site of WDR5 in cells and specifically block interaction of WDR5 with proteins that bind the WIN site. A co-immunoprecipitation (co-IP) for WDR5 in MV4:11 cells treated with DMSO and

16 for 4 h demonstrated reduced binding of MLL1 with WDR5 upon **16** treatment but not DMSO treatment. RBBP5 was used as a control for the specificity of WDR5 WIN site blockade, as RBBP5 is a member of the WRAD complex along with MLL1 but RBBP5 interacts with WDR5 on a binding surface distinct from the WIN site (WBN). Binding of RBBP5 with WDR5 was not affected by compound **16**. Reduced IP of MLL1 but not RBBP5 with WDR5 after **16** treatment indicated that the chemical probe is able to engage the WIN site of WDR5 in live cells and specifically displace protein binding partners that engage at the site.

Detection of Displacement of WDR5 from Chromatin and Transcriptional Repression of WDR5 Bound Genes Leading to p53 Induction.

We previously determined that the primary mechanism of action of our early but moderately potent WDR5 WIN site inhibitor **1** is the rapid displacement of WDR5 from chromatin at a select set of ribosomal protein genes (RPGs) that is conserved across disparate cell types. The displacement of WDR5 from chromatin after compound **1** treatment (2 μ M) is accompanied by a commensurate ~2-fold decrease in mRNA expression of WDR5-bound RPGs.⁸ Thus, we investigated whether our more potent inhibitor **16** can recapitulate the displacement of WDR5 from chromatin and repression of WDR5-bound RPGs as described for **1**.

To investigate WDR5 binding to chromatin after compound **16** treatment, we used chromatin immunoprecipitation (ChIP) to quantify WDR5 enriched at three representative genes that we previously determined to be bound by WDR5 in MV4:11 cells (Figure 5A).⁸ Consistent with our previous report⁸ for **1**, treatment of MV4:11 cells for 4 h with 600 nM **16** resulted in a roughly 90% reduction of WDR5 bound at all three WDR5-bound genes tested. To further assess whether **16** recapitulated the mode of action described for **1**, we next sought to determine whether **16** selectively repressed expression of RPGs at which WDR5 displacement occurs. RT-qPCR analysis revealed that indeed compound **16** reduced expression of both representative WDR5-bound genes tested (*RPS24* and *RPL35*) by roughly 2-fold (Figure 5B). However, expression of two ribosomal protein genes not bound by WDR5 (*RPS11* and *RPL14*),⁸ was not reduced upon **16** treatment. Together, these data indicate that our WDR5 WIN site inhibitors **1** and **16** share a common primary molecular mode of action. Furthermore, compound **16** elicited similar level of cellular response at a significantly lower concentration to compound **1**.

The primary mode of action of our early WIN site inhibitor **1** at 2 μ M (i.e. displacement of WDR5 from chromatin and repression of WDR5 bound genes) leads to induction of a p53-mediated cellular response in cells expressing an oncogenic MLL-fusion.⁸ Thus we sought to determine p53 and p21 protein level changes at 24h and 48h post treatment of compound **16** in MV4:11 cells. Figure 6A depicts the dose dependent elevation of both p53 and p21 proteins in a synchronized manner at both time points, and the effect was maximized at 300 nM concentration of compound **16** then plateaued. A time course analysis revealed that p53 and p21 protein levels started to increase from 8 h post treatment of compound **16** at 300 nM and continued to elevate up to 32 h (Figure 6B). Additionally, compound **16** caused 2.5-fold increase in caspase 3/7 activity in the MLL-fusion cell lines MV4:11 and Molm13 48 h post

treatment (Figure 6C), consistent with induction of apoptosis. Cell cycle analysis of MV4:11 cells treated with 1 μ M compound **16** for 48 hours and subsequently stained with propidium iodide showed an approximate 4 fold increased SubG1 cells, which further supports WDR5 inhibitor mediated induction of apoptosis. G1 and S phase cells had similar levels in both treated and untreated cells, while an apparent decrease in G2M phase cells was observed in compound **16** treated cells (Figure 6D). These data support that all biomarker changes described above are mediated by the inhibition of WDR5 at the WIN site inhibitor by compound **16** and share a common mode of action with our less potent previously described compound **1**.

Displacement of MYC from Chromatin.

Several reports^{8,32} have empirically determined that MLL-fusion leukemia cell lines are sensitive to WIN site inhibition, but we reasoned that WDR5 WIN site inhibitors may have utility in other cancer types as well. We have previously reported that WDR5 facilitates the recruitment of the oncogenic transcription factor MYC to chromatin through a direct interaction.¹⁴ This protein–protein interaction occurs via MYC binding to a surface on WDR5 (the WBN site) that is distinct from the WIN site. Mutations in MYC that disrupt the interaction with WDR5 result in diminished recruitment of MYC to chromatin and impair the ability of MYC to drive tumorigenesis. Therefore, we reasoned that since the WIN site of WDR5 is required for WDR5 engagement with chromatin,⁸ displacement of WDR5 from chromatin by a WIN site inhibitor would also result in displacement of MYC from chromatin, and therefore WIN site inhibition would be effective against MYC driven tumors.

To test this hypothesis, we used ChIP to assess the ability of MYC to engage chromatin at genes that displayed WDR5 displacement upon **16** treatment in Figure 5A. We found that MYC binding to chromatin was also reduced at all three genes tested in response to **16** treatment (Figure 7), indicating that impeding WDR5 associated with chromatin through the WIN site also prevents MYC recruitment to MYC/WDR5 co-bound target genes.

Anti-proliferative Activity of Compound 16 in Other Cancers.

To further assess whether blocking the WIN site of WDR5 by a small molecule can inhibit proliferation in MYC-driven cancers, compound **1** and **16** were tested in cell lines listed in Table 3. Both compounds showed similar cellular selectivity profiles with 10–20 fold higher potency for compound **16** in sensitive cells suggesting the same mechanism of action. CHP-134 (neuroblastoma, wt p53) and Ramos (Burkitt's lymphoma, mutant p53) lines show the highest vulnerability by the WDR5 inhibition at the WIN site among tested cells despite their different p53 status. Compound **16** also exhibited anti-proliferative activities against other Burkitt's lymphoma lines with mutant p53 (Raji and Daudi). In addition, proliferation of the colon cancer line SW620 was moderately inhibited by compound **16** treatment, but SW480 cells were completely resistant. Above results support a potential utility of WDR5 WIN site inhibitors against MYC-driven cancers, and containing wild-type p53 may not be an absolute requirement for a mechanism-based sensitivity. We are currently focused on determining other factors that govern the WDR5 inhibition mediated cellular vulnerability in MYC-upregulated cancers.

WDR5 WIN-site inhibitors were then tested in cancer tissue-originated spheroids (CTOSs), which retain morphological characteristics of the original tumors. Five previously reported colorectal cancer CTOSs^{37,38} with different mutation profiles were treated with compound **1** and **16** (1 and 10 μ M), and dose dependent inhibitions of cell growth were observed in all CTOS lines (Figure 8). Compound **16** exhibited significantly higher potency than **1** as expected. Intriguingly, the C45 line with multiple mutations including p53 was most sensitive by the compound **16** treatment. These results further support a broad utility of WDR5 WIN site inhibitors against solid cancers.

Chemical Synthesis.

Synthesis of compounds **2** – **13** (Scheme 1) began from **23**, which was prepared from a previously reported protocol.³⁹ Boronic pinacol ester **24** was prepared through Miyaura borylation of **23**, and subsequent Suzuki-Miyaura cross-coupling reaction with 2-bromo-5-fluorotoluene gave the biphenyl methyl ester **25**. Carboxylic acid **26** was obtained through hydrolysis of methyl ester **25**. Intermediate **26** underwent amide bond formation with a variety of benzyl amines in a parallel manner to yield benzyl alcohols **27** – **38**. The alcohol functional group of **27** – **38** was then brominated with phosphorus tribromide and then substituted with 1-methyl-2-aminoimidazole to yield compound **2** – **13**.

Preparation of compound **14** – **22** (Scheme 2) began from hemiacetal **39**, which was prepared in three steps from a previously reported protocol.⁴⁰ Compound **39** underwent reductive amination with 2,4-dimethoxybenzylamine to construct the bicyclic core unit of lactam **40**. Triflate **41** was synthesized using *N*-phenylbis(trifluoromethanesulfonimide) and subsequent deprotection of the 2,4-dimethoxybenzyl group gave intermediate **42**. It was then subjected to Suzuki-Miyaura cross-coupling with 2-bromo-5-fluorotoluene to produce biphenyl lactam **43**. Three selected substituted benzyl bromides were introduced at the lactam NH of **43** to yield **44** – **46**. The methyl-2-imidazoleimine group of compound **14** – **16** was introduced from the corresponding intermediate methyl ester **44** – **46** employing three-steps sequence including reduction, bromination and nucleophilic substitution with 1-methyl-2-aminoimidazole. Finally, compound **17** – **22** bearing bioisosteric P₂ units were prepared from bromide **52** by means of nucleophilic substitution with corresponding amines in a parallel manner.

CONCLUSIONS

We describe a novel series of WDR5 WIN site inhibitors containing a bicyclic dihydroisoquinolinone core scaffold that was discovered by structure-guided cyclization of the linear benzamide. This modification fixed the bound conformation and removed a H-bond donor and two rotatable bonds, which resulted in improvements in both on-target potency and drug-like properties. The most potent WDR5 inhibitor compound **16** exhibited a picomolar binding affinity and clinically relevant anti-proliferative activities with enhanced selectivity in the MLL-fusion cell lines MV4:11 and Molm13. Compound **16** also effectively displaced WDR5 from chromatin, which led to the dose-dependent induction of p53 followed by caspase3/7 in the MLL-fusion cells.

A potential utility of WDR5 WIN site inhibitors in MYC-driven cancers was also assessed using compound **16** because displacement of WDR5 from chromatin also prevents MYC recruitment to MYC/WDR5 co-bound target genes. Indeed, compound **16** diminished MYC recruitment at WDR5-displaced genes and exhibited potent anti-proliferative effects in CHP-134 (neuroblastoma) and Ramos (Burkitt's lymphoma) lines.

The observations that WDR5 WIN site inhibition impedes not only WDR5 but also MYC binding to chromatin, and prevents proliferation of MYC driven cell lines have tremendous therapeutic implications. MYC over-expression or dysregulation is found in the majority of cancers and contributes to an estimated 100,000 cancer-related deaths in the United States each year.⁴¹ Despite the known contributions of MYC function to cancer, MYC had long been considered “undruggable”. Our data presented here predicts that MYC can be indirectly therapeutically targeted in cancer via WDR5 WIN site inhibition at genes co-bound by WDR5 and MYC. Although the number of WDR5 target genes we recently identified in MV4:11 cells is fairly small, these genes are highly enriched in genes encoding components of the protein synthesis machinery.⁸ Enhanced protein synthesis is a core tumorigenic activity of MYC,⁴² and thus we predict that WDR5 WIN site inhibitors should effectively block this tumorigenic function of MYC by preventing MYC recruitment to a key set of protein synthesis genes.

In summary, this study demonstrates the successful targeting of WDR5 by structure-guided methods to produce a set of high-affinity WDR5 WIN-site inhibitors. Current efforts are focused on further optimization of the potency, pharmaceutical, and pharmacokinetic properties of this series to obtain candidates that are suitable for clinical development. In addition, we are expanding our understanding in mechanisms of action, cellular vulnerability and additional utility of WDR5 WIN site inhibitors.

EXPERIMENTAL SECTION

General Chemistry.

All chemical reagents and reaction solvents were purchased from commercial suppliers and used as received. Proton nuclear magnetic resonance (¹H NMR) and carbon nuclear magnetic resonance (¹³C NMR) spectra were recorded on either a 400, 600 or 800 MHz Bruker spectrometer. For ¹H NMR spectra, chemical shifts are reported in parts per million (ppm) and are reported relative to residual nondeuterated solvent signals. Coupling constants are reported in hertz (Hz). The following abbreviations (or a combination, thereof) are used to describe splitting patterns: s, singlet; d, doublet; t, triplet; q, quartet; quint, quintet; m, multiplet; comp, overlapping multiplets of nonmagnetically equivalent protons; br, broad. All final compounds were of 95% purity or higher as measured by analytical reversed-phase HPLC. Analytical HPLC was performed on an Agilent 1200 series system with UV detection at 214 and 254 nm, along with evaporative light scattering detection (ELSD). Low-resolution mass spectra were obtained on an Agilent 6140 mass spectrometer with electrospray ionization (ESI). LC-MS experiments were performed with the following parameters: Phenomenex Kinetex 2.6 μm XB-C18 100 Å LC column (50 mm × 2.1 mm); 2 min gradient, 5%–95% MeCN in H₂O, and 0.1% TFA or 0.1% formic acid. Analytical thin layer chromatography (TLC) was performed on Kieselgel 60 F254 glass plates precoated

with a 0.25 mm thickness of silica gel. TLC plates were visualized with UV light and iodine. Silica gel chromatography was performed using a Teledyne ISCO Combiflash R_f system, eluting with varying concentrations of EtOAc in hexanes or MeOH in CH₂Cl₂. Preparative reversed-phase HPLC was performed on a Gilson HPLC equipped with a Phenomenex Kinetex C18 column, using varying concentrations of MeCN in H₂O, and 0.1% TFA. Solvents for reactions, extraction, and washing were ACS grade, and solvents for chromatography were HPLC grade. Compounds **1**, **23**, and **39** were prepared according to previously reported protocols.^{8,39,40}

General Procedure A: amide coupling.

The carboxylic acid (1.0 equiv.) was taken up in DMF (0.8 mL) and then *N,N,N',N'*-Tetramethyl-*O*-(benzotriazol-1-yl)uronium tetrafluoroborate (1.0 equiv.) and *N,N*-diisopropylethylamine (2.0 equiv.) were added, after stirring at room temperature for 10 min R¹-benzyl amine (1.0 equiv.) was added. After stirring for 8 h at room temperature the reaction was diluted with EtOAc (5 mL) and washed with 1 M HCl (5 mL), sat. NaHCO₃ (5 mL), water (5 mL) and brine (5 mL). The organic layer was then dried (MgSO₄), filtered and concentrated. The crude residue was purified by silica gel chromatography (0 – 75% EtOAc:hexanes).

General Procedure B: bromination and 1-methyl-2-aminoimidazole addition.

The benzyl alcohol (1.0 equiv.) was taken up in CH₂Cl₂ (1.1 mL) and then PBr₃ (3.0 equiv.) was added. The reaction was stirred at room temperature for 2 h and then sat. NaHCO₃ (5 mL) was added. The layers were separated and the aqueous layer was extracted with CH₂Cl₂ (3 × 5 mL). The combined organic layers were washed with brine (5 mL), dried (MgSO₄), filtered and concentrated. The residue was taken up in MeCN (0.75 mL) and then 1-methyl-2-aminoimidazole hydrochloride salt (3.0 equiv.), *N,N*-diisopropylethylamine (3.0 equiv.) and potassium iodide (0.1 equiv.) were added. The reaction was heated at 80 °C for 4 h and then cooled to room temperature and diluted with water (5 mL). The aqueous layer was extracted with EtOAc (3 × 5 mL) and the combined organic layers were washed with brine (5 mL), dried (MgSO₄), filtered and concentrated. The residue was purified by reverse phase HPLC (Phenomenex Gemini C18, H₂O:CH₃CN gradient from 15–95% CH₃CN, 0.1% TFA). The product was dissolved in CH₂Cl₂ and washed with sat. K₂CO₃ to remove TFA.

General procedure C: benzylation of methyl 5-(4-fluoro-2-methylphenyl)-1-oxo-1,2,3,4-tetrahydroisoquinoline-7-carboxylate.

To a solution of lactam (1 equiv.) in DMF at 0 °C was added NaH (60% in mineral oil, 1.3 equiv.). After stirring for 15 min, the substituted R²-benzyl halide (1.3 equiv.) was added and the mixture was stirred for 1 h and quenched with saturated aqueous NH₄Cl. The mixture was extracted with EtOAc, and the organic layer was dried (Na₂SO₄) and concentrated. The residue was purified by silica gel chromatography (0 – 100% EtOAc:hexanes).

General procedure D: reduction of methyl ester.

To a solution of methyl ester (1 equiv.) in THF at 0 °C was added dropwise 3 M solution of LiBHET₃ in THF (3 equiv.). The reaction was stirred for 30 min and quenched with sat.

NaHCO₃. The mixture was extracted with EtOAc, and the organic layer was dried (Na₂SO₄) and concentrated. The residue was purified by silica gel chromatography (0 – 100% EtOAc:hexanes).

General procedure E: bromination of benzyl alcohol.

To a solution of benzyl alcohol (1 equiv.) in CH₂Cl₂ at 0 °C was added a 1 M solution of PBr₃ in CH₂Cl₂ (2 equiv.) dropwise. The reaction was stirred for 4 h, then quenched with sat. NaHCO₃. The mixture was extracted with Et₂O. The organic layer was dried (Na₂SO₄) and concentrated. The residue was purified by silica gel chromatography (0 – 100% EtOAc:hexanes).

General procedure F: displacement of benzyl bromide with amine.

A mixture of benzyl bromide (1 equiv.), R³-imidazole amine (3 equiv.), KI (1 equiv.), and *N,N*-diisopropylethylamine (3 equiv.) was stirred at 50 °C for 16 h. The solvent was removed under reduced pressure and the residue was purified by reverse phase HPLC (Phenomenex Gemini C18, H₂O:CH₃CN gradient from 15–95% CH₃CN, 0.1% TFA). The product was dissolved in CH₂Cl₂ and washed with sat. aq. K₂CO₃ to remove TFA.

N-Benzyl-4'-fluoro-5-((2-imino-3-methyl-2,3-dihydro-1*H*-imidazol-1-yl)methyl)-2'-methyl-[1,1'-biphenyl]-3-carboxamide (2).

General procedure B was followed using **27** (25 mg, 0.07 mmol) to obtain the title compound (7.1 mg, 23% yield). ¹H NMR (400 MHz, MeOD) δ 7.76 (d, *J* = 4.8 Hz, 1H), 7.37 – 7.32 (m, 5H), 7.28 – 7.22 (m, 2H), 7.08 (dd, *J* = 10.0, 2.8 Hz, 1H), 7.02 – 6.99 (m, 1H), 6.63 (d, *J* = 8.4 Hz, 1H), 5.04 (s, 2H), 4.60 (s, 2H), 3.35 (s, 3H), 2.24 (s, 3H); ¹³C NMR (200 MHz, MeOD) δ 169.5, 163.9 (d, *J* = 244.0 Hz), 152.6, 143.6, 140.2, 139.4 (d, *J* = 8.0 Hz), 138.2 (d, *J* = 3.0 Hz), 138.1, 136.6, 132.5 (d, *J* = 8.0 Hz), 129.7, 128.9, 128.7, 128.4, 126.4, 118.0 (d, *J* = 20.0 Hz), 116.8, 114.9, 113.8 (d, *J* = 20.0 Hz), 49.6, 44.8, 32.6, 20.8; LCMS (ESI): *m/z* = 429.0 [M + H]⁺.

4'-Fluoro-5-((2-imino-3-methyl-2,3-dihydro-1*H*-imidazol-1-yl)methyl)-2'-methyl-*N*-(3-methylbenzyl)-[1,1'-biphenyl]-3-carboxamide (3).

General procedure B was followed using **28** (30 mg, 0.08 mmol) to obtain the title compound (8.9 mg, 24% yield). ¹H NMR (400 MHz, MeOD) δ 7.86 (s, 1H), 7.77 (s, 1H), 7.70 (s, 1H), 7.49 (s, 1H), 7.27 – 7.20 (m, 4H), 7.17 (d, *J* = 6.4 Hz, 1H), 7.09 – 6.98 (m, 2H), 6.77 (d, *J* = 8.0 Hz, 1H), 4.73 (s, 2H), 4.56 (d, *J* = 2.8 Hz, 2H), 2.34 (s, 3H), 2.27 (s, 3H), 2.24 (s, 3H); ¹³C NMR (200 MHz, MeOD) δ 170.0, 163.8 (d, *J* = 244.0 Hz), 152.6, 143.8, 140.2, 139.4, 138.7 (d, *J* = 8.0 Hz), 136.9 (d, *J* = 3.0 Hz), 136.0, 132.5 (d, *J* = 8.0 Hz), 132.1, 129.6, 129.4, 129.0, 128.2, 125.8, 125.6, 118.4, 117.9 (d, *J* = 20.0 Hz), 116.5, 113.7 (d, *J* = 20.0 Hz), 64.8, 49.5, 44.7, 21.6, 20.8; LCMS (ESI): *m/z* = 443.1 [M + H]⁺.

N-(3-Chlorobenzyl)-4'-fluoro-5-((2-imino-3-methyl-2,3-dihydro-1*H*-imidazol-1-yl)methyl)-2'-methyl-[1,1'-biphenyl]-3-carboxamide (4).

General procedure B was followed using **29** (34 mg, 0.09 mmol) to obtain the title compound (10.8 mg, 26% yield). ¹H NMR (400 MHz, MeOD) δ 7.77 (s, 1H), 7.76 (s, 1H),

7.38 (s, 1H), 7.36 – 7.23 (m, 5H), 7.08 – 6.97 (m, 2H), 6.67–6.63 (m, 2H), 5.07 (s, 2H), 4.58 (s, 2H), 3.37 (s, 3H), 2.25 (s, 3H); ^{13}C NMR (200 MHz, MeOD) δ 169.5, 163.9 (d, J = 244.0 Hz), 152.3, 143.6, 142.7, 139.4 (d, J = 8.0 Hz), 138.1 (d, J = 3.0 Hz), 136.4, 135.5, 132.7, 132.5 (d, J = 8.0 Hz), 131.2, 128.9, 128.7, 128.5, 127.1, 126.4, 118.0 (d, J = 20.0 Hz), 116.9, 115.0, 113.9 (d, J = 20.0 Hz), 49.5, 44.2, 32.6, 20.81 LCMS (ESI): m/z = 463.0 [M + H] $^{+}$.

***N*-(3-Methoxybenzyl)-4'-fluoro-5-((2-imino-3-methyl-2,3-dihydro-1*H*-imidazol-1-yl)methyl)-2'-methyl-[1,1'-biphenyl]-3-carboxamide (5).**

General procedure B was followed using **30** (58 mg, 0.15 mmol) to obtain the title compound (21.0 mg, 30% yield). ^1H NMR (400 MHz, DMSO- d_6) δ 9.05 (t, J = 6.0 Hz, 1H), 7.80 (s, 1H), 7.74 (s, 1H), 7.38 (s, 1H), 7.29 – 7.17 (series of m, 3H), 7.11 (dt, J = 8.6, 2.9 Hz, 1H), 6.90 – 6.87 (m, 2H), 6.82 – 6.79 (m, 1H), 6.45 (d, J = 2.7 Hz, 1H), 6.35 (d, J = 2.7 Hz, 1H), 4.81 (s, 2H), 4.44 (d, J = 6.0 Hz, 2H), 3.72 (s, 3H), 3.06 (s, 3H), 2.21 (s, 3H); ^{13}C NMR (150 MHz, DMSO- d_6) δ 166.3, 161.9 (d, J = 242.5 Hz), 159.7, 153.6, 141.6, 140.7, 139.0, 138.2 (d, J = 8.0 Hz), 137.3 (d, J = 3.2 Hz), 135.1, 131.9 (d, J = 8.0 Hz), 137.3 (d, J = 3.2 Hz), 135.1, 131.9 (d, J = 8.0 Hz), 131.4, 129.8, 126.8, 126.0, 119.9, 117.3 (d, J = 21.0 Hz), 113.6, 113.5, 113.2 (d, J = 21.0 Hz), 112.5, 111.9, 55.4, 47.1, 43.1, 31.5, 20.7; LCMS (ESI): m/z = 459.5 [M + H] $^{+}$.

4'-Fluoro-5-((2-imino-3-methyl-2,3-dihydro-1*H*-imidazol-1-yl)methyl)-2'-methyl-*N*-(3-(trifluoromethoxy)benzyl)-[1,1'-biphenyl]-3-carboxamide (6).

General procedure B was followed using **31** (38 mg, 0.09 mmol) to obtain the title compound (10.4 mg, 23% yield). ^1H NMR (400 MHz, MeOD) δ 7.87 (s, 1H), 7.71 (s, 1H), 7.50 (s, 1H), 7.47 – 7.38 (m, 2H), 7.29 – 7.24 (m, 2H), 7.19 (d, J = 7.6 Hz, 1H), 7.08 – 7.05 (m, 2H), 7.02 – 6.98 (m, 2H), 4.74 (s, 2H), 4.63 (s, 2H), 3.37 (s, 3H), 2.27 (s, 3H); ^{13}C NMR (200 MHz, MeOD) δ 170.1, 163.8 (d, J = 244.0 Hz), 150.9, 143.9, 143.3, 143.1, 139.3 (d, J = 8.0 Hz), 138.7 (d, J = 3.0 Hz), 135.7, 132.5 (d, J = 8.0 Hz), 132.2, 131.4, 128.2, 127.4, 125.6, 122.7, 121.4, 121.2, 120.7, 117.9 (d, J = 20.0 Hz), 113.7 (d, J = 20.0 Hz), 64.8, 49.5, 44.1, 20.8; LCMS (ESI): m/z = 513.0 [M + H] $^{+}$.

***N*-(3,4-Dichlorobenzyl)-4'-fluoro-5-((2-imino-3-methyl-2,3-dihydro-1*H*-imidazol-1-yl)methyl)-2'-methyl-[1,1'-biphenyl]-3-carboxamide (7).**

General procedure B was followed using **32** (35 mg, 0.08 mmol) to obtain the title compound (8.8 mg, 21% yield). ^1H NMR (400 MHz, MeOD) δ 7.81 (s, 1H), 7.78 (s, 1H), 7.53 (d, J = 1.6 Hz, 1H), 7.51 (d, J = 8.4 Hz, 1H), 7.41 (s, 1H), 7.31 – 7.24 (m, 2H), 7.10 (dd, J = 9.6, 2.4 Hz, 1H), 7.04 – 6.96 (m, 3H), 5.24 (s, 2H), 4.56 (s, 2H), 3.56 (s, 3H), 2.25 (s, 3H); ^{13}C NMR (200 MHz, MeOD) δ 169.3, 163.9 (d, J = 244.0 Hz), 147.9, 143.9, 141.2, 139.4 (d, J = 8.0 Hz), 137.9 (d, J = 3.0 Hz), 136.8, 136.4, 132.7, 132.5 (d, J = 8.0 Hz), 132.2, 131.8, 130.8, 129.1, 128.7, 126.6, 118.9, 118.1 (d, J = 20.0 Hz), 116.9, 113.9 (d, J = 20.0 Hz), 49.5, 43.7, 33.4, 20.8; LCMS (ESI): m/z = 497.4 [M + H] $^{+}$.

***N*-(4-Chloro-3-methylbenzyl)-4'-fluoro-5-((2-imino-3-methyl-2,3-dihydro-1*H*-imidazol-1-yl)methyl)-2'-methyl-[1,1'-biphenyl]-3-carboxamide (8).**

General procedure B was followed using **33** (32 mg, 0.08 mmol) to obtain the title compound (9.6 mg, 25% yield). ¹H NMR (400 MHz, MeOD) δ 7.80 (s, 1H), 7.78 (s, 1H), 7.40 (s, 1H), 7.32 – 7.23 (m, 2H), 7.18 (d, *J* = 8.0 Hz, 1H), 7.09 (d, *J* = 2.4 Hz, 1H), 7.07 (d, *J* = 2.4 Hz, 1H), 7.03–6.96 (m, 3H), 5.24 (s, 2H), 4.54 (s, 2H), 3.56 (s, 3H), 2.36 (s, 3H), 2.25 (s, 3H); ¹³C NMR (200 MHz, MeOD) δ 169.2, 164.0 (d, *J* = 244.0 Hz), 147.9, 143.8, 139.4 (d, *J* = 8.0 Hz), 139.1, 138.0 (d, *J* = 3.0 Hz), 137.3, 136.7, 136.6, 134.2, 132.6 (d, *J* = 8.0 Hz), 131.5, 130.2, 129.2, 127.8, 126.5, 118.8, 118.0 (d, *J* = 20.0 Hz), 116.9, 113.9 (d, *J* = 20.0 Hz), 49.8, 44.1, 33.4, 20.8, 20.2; LCMS: *m/z* = 477.4 [M + H]⁺.

***N*-(3-Methyl,-4-fluorobenzyl)-4'-fluoro-5-((2-imino-3-methyl-2,3-dihydro-1*H*-imidazol-1-yl)methyl)-2'-methyl-[1,1'-biphenyl]-3-carboxamide (9).**

General procedure B was followed using **34** (83 mg, 0.22 mmol) to obtain the title compound (28.0 mg, 28% yield). ¹H NMR (400 MHz, DMSO-*d*₆) δ 9.05 (t, *J* = 6.0 Hz, 1H), 7.80 (s, 1H), 7.73 (s, 1H), 7.38 (s, 1H), 7.28 – 7.04 (series of m, 6H), 6.42 (d, *J* = 2.7 Hz, 1H), 6.32 (d, *J* = 2.7 Hz, 1H), 4.79 (s, 2H), 4.41 (d, *J* = 6.0 Hz, 2H), 3.04 (s, 3H), 2.21 (s, 3H), 2.20 (s, 3H); ¹³C NMR (150 MHz, DMSO-*d*₆) δ 166.2, 161.9 (d, *J* = 242.4 Hz), 160.1 (d, *J* = 240.0 Hz), 153.9, 140.7, 139.1, 138.2 (d, *J* = 7.9 Hz), 137.3 (d, *J* = 2.2 Hz), 135.9 (d, *J* = 3.1 Hz), 135.0, 131.9 (d, *J* = 8.3 Hz), 131.5, 131.0 (d, *J* = 4.8 Hz), 127.0 (d, *J* = 8.1 Hz), 126.8, 126.0, 124.3 (d, *J* = 17.0 Hz), 117.3 (d, *J* = 21.0 Hz), 115.1 (d, *J* = 22.0 Hz), 113.3, 113.2 (d, *J* = 21.0 Hz), 111.7, 47.1, 42.5, 31.4, 20.7, 14.6; LCMS (ESI): *m/z* = 461.4 [M + H]⁺.

***N*-(3-Methoxy,-4-fluorobenzyl)-4'-fluoro-5-((2-imino-3-methyl-2,3-dihydro-1*H*-imidazol-1-yl)methyl)-2'-methyl-[1,1'-biphenyl]-3-carboxamide (10).**

General procedure B was followed using **35** (38 mg, 0.09 mmol) to obtain the title compound (18.0 mg, 40% yield). ¹H NMR (400 MHz, DMSO-*d*₆) δ 9.04 (t, *J* = 5.7 Hz, 1H), 7.80 (s, 1H), 7.73 (s, 1H), 7.38 (s, 1H), 7.28 – 7.24 (m, 1H), 7.20 – 7.08 (series of m, 4H), 6.88 – 6.85 (m, 1H), 6.43 (d, *J* = 2.6 Hz, 1H), 6.34 (d, *J* = 2.6 Hz, 1H), 4.80 (s, 2H), 4.44 (d, *J* = 5.7 Hz, 2H), 3.81 (s, 3H), 3.05 (s, 3H), 2.21 (s, 3H); ¹³C NMR (150 MHz, DMSO-*d*₆) δ 166.3, 161.94 (d, *J* = 242.6 Hz), 153.9, 151.0 (d, *J* = 241.0 Hz), 147.3 (d, *J* = 10.6 Hz), 140.7, 139.2, 138.2 (d, *J* = 8.0 Hz), 137.3 (d, *J* = 2.2 Hz), 136.8 (d, *J* = 3.3 Hz), 135.1, 131.9 (d, *J* = 8.4 Hz), 131.5, 126.8, 126.0, 119.9 (d, *J* = 6.7 Hz), 117.3 (d, *J* = 21.0 Hz), 116.0 (d, *J* = 17.8 Hz), 113.5, 113.3, 113.2 (d, *J* = 21.0 Hz), 111.6, 56.3, 47.1, 42.8, 31.4, 20.7; LCMS (ESI): *m/z* = 477.0 [M + H]⁺.

***N*-(3,5-Dimethylbenzyl)-4'-fluoro-5-((2-imino-3-methyl-2,3-dihydro-1*H*-imidazol-1-yl)methyl)-2'-methyl-[1,1'-biphenyl]-3-carboxamide (11).**

General procedure B was followed using **36** (94 mg, 0.25 mmol) to obtain the title compound (8 mg, 7% yield). ¹H NMR (400 MHz, DMSO-*d*₆) δ 9.01 (t, *J* = 5.8 Hz, 1H), 7.81 (s, 1H), 7.74 (s, 1H), 7.38 (s, 1H), 7.29 – 7.25 (m, 1H), 7.18 (dd, *J* = 10.1, 2.5 Hz, 1H), 7.11 (dt, *J* = 8.6, 2.7 Hz, 1H), 6.91 (s, 2H), 6.86 (s, 1H), 6.44 (d, *J* = 2.8 Hz, 1H), 6.34 (d, *J* = 2.8 Hz, 1H), 4.80 (s, 2H), 4.40 (d, *J* = 5.8 Hz, 2H), 3.05 (s, 3H), 2.23 (s, 6H), 2.21 (s, 3H).

^{13}C NMR (150 MHz, DMSO- d_6) δ 166.1, 161.9 (d, J = 242.6 Hz), 153.9, 140.6, 139.9, 139.1, 138.2 (d, J = 8.3 Hz), 137.7, 137.3 (d, J = 2.8 Hz), 135.1, 131.9 (d, J = 8.3 Hz), 131.4, 128.6, 126.8, 126.1, 125.6, 117.3 (d, J = 21.0 Hz), 113.3, 113.2 (d, J = 20.8 Hz), 111.7, 47.1, 43.1, 31.4, 21.4, 20.7; LCMS (ESI): m/z = 457.0 [M + H] $^+$.

***N*-(3,5-Dichlorobenzyl)-4'-fluoro-5-((2-imino-3-methyl-2,3-dihydro-1*H*-imidazol-1-yl)methyl)-2'-methyl-[1,1'-biphenyl]-3-carboxamide (12).**

General procedure B was followed using **37** (112 mg, 0.27 mmol) to obtain the title compound (12 mg, 9% yield). ^1H NMR (400 MHz, DMSO- d_6) δ 9.01 (t, J = 5.4 Hz, 1H), 7.81 (s, 1H), 7.74 (s, 1H), 7.49 (s, 1H), 7.40 (s, 1H), 7.36 (s, 2H), 7.29 – 7.25 (m, 1H), 7.19 – 7.17 (m, 1H), 7.14 – 7.09 (m, 1H), 6.46 (d, J = 1.5 Hz, 1H), 6.36 (d, J = 1.5 Hz, 1H), 4.82 (s, 2H), 4.47 (d, J = 5.4 Hz, 2H), 3.06 (s, 3H), 2.21 (s, 3H); ^{13}C NMR (150 MHz, DMSO- d_6) δ 166.5, 161.9 (d, J = 242.7 Hz), 153.6, 144.5, 140.8, 139.1, 138.2 (d, J = 8.2 Hz), 137.2 (d, J = 2.6 Hz), 134.7, 134.4, 131.9 (d, J = 8.4 Hz), 131.7, 126.9, 126.8, 126.6, 126.0, 117.3 (d, J = 21.0 Hz), 113.5, 113.2 (d, J = 21.0 Hz), 111.8, 47.1, 42.4, 31.4, 20.7; LCMS (ESI): m/z = 496.9 [M + H] $^+$.

***N*-(3,5-Dimethoxybenzyl)-4'-fluoro-5-((2-imino-3-methyl-2,3-dihydro-1*H*-imidazol-1-yl)methyl)-2'-methyl-[1,1'-biphenyl]-3-carboxamide (13).**

General procedure B was followed using **38** (84 mg, 0.20 mmol) to obtain the title compound (12 mg, 12% yield). ^1H NMR (400 MHz, CDCl_3) δ 7.76 (s, 1H), 7.3 (s, 1H), 7.27 (s, 1H), 7.15 – 7.11 (m, 1H), 6.97 – 6.89 (m, 2H), 6.79 – 6.74 (m, 1H), 6.97 – 6.89 (m, 2H), 6.79 – 6.74 (m, 1H), 6.50 (d, J = 7.4 Hz, 2H), 6.36 (t, J = 2.2 Hz, 1H), 6.14 – 6.12 (m, 2H), 4.86 (s, 2H), 4.57 (d, J = 5.4 Hz, 2H), 3.77 (s, 6H), 3.24 (s, 3H), 2.20 (s, 3H); ^{13}C NMR (150 MHz, CDCl_3) δ 166.7, 162.2 (d, J = 244 Hz), 161.0, 142.1, 140.8, 137.7 (d, J = 7.9 Hz), 136.4 (d, J = 3.3 Hz), 135.5, 135.2, 131.3, 131.2 (d, J = 7.9 Hz), 128.4, 125.7, 116.9 (d, J = 21.0 Hz), 115.1, 113.1, 112.8 (d, J = 21.0 Hz), 105.9, 105.7, 99.3, 55.4, 48.9, 43.9, 33.0, 20.6; LCMS: m/z = 489.5 [M + H] $^+$.

2-(4-Chloro-3-methylbenzyl)-5-(4-fluoro-2-methylphenyl)-7-((2-imino-3-methyl-2,3-dihydro-1*H*-imidazol-1-yl)methyl)-3,4-dihydroisoquinolin-1(2*H*)-one (14).

General procedure F was followed using **50** (30 mg, 0.06 mmol) and 1-methyl-1*H*-imidazol-2-amine hydrochloride (25 mg, 0.18 mmol) to obtain the title compound (25 mg, 81% yield). ^1H NMR (400 MHz, CDCl_3) δ 8.06 (d, J = 1.6 Hz, 1H), 7.29 (m, 1H), 7.25 (d, J = 1.6 Hz, 1H), 7.20 (s, 1H), 7.09 (dd, J = 2.0, 8.0 Hz, 1H), 7.03 (dd, J = 6.4, 8.4 Hz, 1H), 6.97 (dd, J = 2.4, 9.6 Hz, 1H), 6.91 (dt, J = 2.4, 8.4 Hz, 1H), 6.20 (m, 2H), 4.97 (s, 2H), 4.72 (ABq, J_{AB} = 14.8 Hz, 2H), 3.37 (t, J = 6.4 Hz, 2H), 3.33 (s, 3H), 2.56 (m, 2H), 2.36 (s, 3H), 2.03 (s, 3H); ^{13}C NMR (100 MHz, CDCl_3) δ 164.4, 162.4 (d, J = 244.0 Hz), 153.0, 139.7, 138.5 (d, J = 8.0 Hz), 136.5, 136.1, 135.9, 135.2, 135.0, 133.7, 132.5, 131.0 (d, J = 8.0 Hz), 130.8, 130.3, 129.4, 127.0 (d, J = 3.0 Hz), 116.8 (d, J = 21.0 Hz), 114.0, 112.8 (d, J = 21.0 Hz), 112.1, 50.1, 48.4, 45.3, 32.4, 25.7, 20.3, 20.2; LCMS (ESI): >95%, m/z = 503.4 [M + H] $^+$.

5-(4-Fluoro-2-methylphenyl)-2-(4-fluoro-3-methylbenzyl)-7-((2-imino-3-methyl-2,3-dihydro-1H-imidazol-1-yl)methyl)-3,4-dihydroisoquinolin-1(2H)-one (15).

General procedure F was followed using **51** (35 mg, 0.07 mmol) and 1-methyl-1H-imidazol-2-amine hydrochloride (30 mg, 0.22 mmol) to obtain the title compound (18 mg, 50% yield). ¹H NMR (400 MHz, CDCl₃) δ 8.04 (d, *J* = 1.3 Hz, 1H), 7.16 (d, *J* = 1.5 Hz, 1H), 7.13 (d, *J* = 7.3 Hz, 1H), 7.10 – 7.07 (m, 1H), 7.01 – 6.98 (m, 1H), 6.95 – 6.86 (m, 3H), 6.09 (s, 2H), 4.81 (s, 2H), 4.68 (ABq, *J*_{AB} = 14.6 Hz, 2H), 3.72 (brs, 1H), 3.33 (t, *J* = 6.6 Hz, 1H), 3.20 (s, 3H), 2.62 – 2.45 (m, 2H), 2.22 (s, 3H), 2.00 (s, 3H); ¹³C NMR (100 MHz, CDCl₃) δ 164.4, 162.2 (d, *J* = 244.5 Hz), 160.9 (d, *J* = 243.0 Hz), 154.6, 139.6, 138.5 (d, *J* = 7.8 Hz), 135.8 (d, *J* = 6.4 Hz), 135.1 (d, *J* = 3.1 Hz), 132.8 (d, *J* = 3.5 Hz), 132.1, 131.4 (d, *J* = 5.2 Hz), 131.0 (d, *J* = 8.2 Hz), 130.3, 127.1 (d, *J* = 8.1 Hz), 126.8, 125.3 (d, *J* = 17.5 Hz), 116.8 (d, *J* = 21.0 Hz), 115.8 (d, *J* = 22.5 Hz), 113.2, 112.8 (d, *J* = 21.1 Hz), 111.2, 50.0, 47.9, 45.2, 31.7, 25.6, 20.2, 14.6 (d, *J* = 3.5 Hz); LCMS (ESI): >95%, *m/z* = 487.6 [M + H]⁺.

2-(3,5-Dimethoxybenzyl)-5-(4-fluoro-2-methylphenyl)-7-((2-imino-3-methyl-2,3-dihydro-1H-imidazol-1-yl)methyl)-3,4-dihydroisoquinolin-1(2H)-one (16).

General procedure F was followed using **52** (30 mg, 0.06 mmol) and 1-methyl-1H-imidazol-2-amine hydrochloride (24 mg, 0.18 mmol) to obtain the title compound (20 mg, 66% yield). ¹H NMR (400 MHz, CDCl₃) δ 8.03 (d, *J* = 2.0 Hz, 1H), 7.31 (d, *J* = 2.0 Hz, 1H), 7.91 (m, 3H), 6.48 (dd, *J* = 4.8, 2.8 Hz, 2H), 6.44 (d, *J* = 2.0 Hz, 2H), 6.37 (t, *J* = 2.0 Hz, 1H), 5.28 (s, 2H), 4.66 (ABq, *J*_{AB} = 14.8 Hz, 2H), 3.76 (s, 6H), 3.60 (s, 3H), 3.38 (t, *J* = 6.4 Hz, 2H), 2.54 (m, 2H), 2.03 (s, 3H); ¹³C NMR (100 MHz, CDCl₃) δ 164.4, 162.3 (d, *J* = 244.8 Hz), 161.2, 152.7, 139.7, 139.6, 138.5 (d, *J* = 7.9 Hz), 136.1, 135.1, 135.0 (d, *J* = 3.1 Hz), 132.6, 131.0 (d, *J* = 8.4 Hz), 130.3, 129.4, 127.2, 116.7 (d, *J* = 20.9 Hz), 114.1, 112.7 (d, *J* = 21.0 Hz), 112.0, 106.2, 99.4, 55.5, 50.6, 48.3, 45.1, 32.3, 25.7, 20.2; LCMS (ESI): >95%, *m/z* = 515.0 [M + H]⁺.

7-((3-Cyclopropyl-2-imino-2,3-dihydro-1H-imidazol-1-yl)methyl)-2-(3,5-dimethoxybenzyl)-5-(4-fluoro-2-methylphenyl)-3,4-dihydroisoquinolin-1(2H)-one (17).

General procedure F was followed using **52** (28 mg, 0.06 mmol) and 1-cyclopropyl-1H-imidazol-2-amine (17.3 mg, 0.14 mmol) to obtain the title compound (24 mg, 79% yield). ¹H NMR (400 MHz, CDCl₃) δ 8.04 (d, *J* = 2.0 Hz, 1H), 7.26 (d, *J* = 2.0 Hz, 1H), 7.02 (dd, *J* = 6.0, 8.4 Hz, 1H), 6.95 (dd, *J* = 2.8, 10.0 Hz, 1H), 6.91 (m, 1H), 6.46 (d, *J* = 2.0 Hz, 2H), 6.36 (m, 1H), 6.15 (d, *J* = 2.8 Hz, 1H), 6.09 (d, *J* = 2.8 Hz, 1H), 5.00 (s, 2H), 4.70 (ABq, *J*_{AB} = 14.8 Hz, 2H), 3.76 (s, 6H), 3.36 (t, *J* = 6.4 Hz, 2H), 2.84 (m, 1H), 2.53 (m, 2H), 2.01 (s, 3H), 1.01 (m, 2H), 0.87 (m, 2H); ¹³C NMR (100 MHz, CDCl₃) δ 164.5, 162.4 (d, *J* = 245.0 Hz), 161.2, 154.0, 139.8, 139.6, 138.5 (d, *J* = 8.0 Hz), 136.1, 135.4, 135.1, 132.7, 131.0 (d, *J* = 8.0 Hz), 130.3, 127.1, 116.8 (d, *J* = 21.0 Hz), 113.0, 112.8 (d, *J* = 21.0 Hz), 111.8, 106.2, 99.5, 55.5, 50.7, 48.1, 45.1, 25.9, 25.7, 20.3, 6.4; LCMS (ESI): >95%, *m/z* = 541.6 [M+H]⁺.

***N*-((2-(3,5-Dimethoxybenzyl)-5-(4-fluoro-2-methylphenyl)-1-oxo-1,2,3,4-tetrahydroisoquinolin-7-yl)methyl)cyclopropanecarboximidamide (18).**

General procedure F was followed using **52** (35 mg, 0.07 mmol) and cyclopropanecarboximidamide hydrochloride (25 mg, 0.21 mmol) to obtain the title compound (12 mg, 35% yield). ¹H NMR (400 MHz, CDCl₃) δ 8.13 (d, *J*=1.6 Hz, 1H), 7.26 (m, 1H), 7.03 (dd, *J*= 6.0, 8.4 Hz, 1H), 6.97 (dd, *J*= 2.4, 9.6 Hz, 1H), 6.91 (dt, *J*= 2.4, 8.4 Hz, 1H), 6.47 (d, *J*= 2.0 Hz, 2H), 6.37 (t, *J*= 2.4 Hz, 1H), 4.72 (ABq, *J*_{AB} = 14.8 Hz, 2H), 4.48 (brs, 2H), 3.77 (s, 6H), 3.37 (t, *J*= 6.4 Hz, 2H), 2.56 (m, 2H), 2.05 (s, 3H), 1.44 (m, 1H), 0.8 (m, 4H); ¹³C NMR (150 MHz, CDCl₃) δ 164.7, 162.9, (d, *J*= 245.0 Hz), 161.2, 139.9, 139.3, 138.5 (d, *J*= 7.5 Hz), 135.4, 132.4, 131.0 (d, *J*= 7.5 Hz), 130.2, 126.8, 116.8 (d, *J*= 21.0 Hz), 112.8 (*J*= 21.0 Hz), 106.2, 99.5, 55.5, 50.7, 45.3, 29.9, 25.7, 20.3, 15.7, 6.7; LCMS (ESI): >95%, *m/z* = 502.6 [M + H]⁺.

2-(3,5-Dimethoxybenzyl)-5-(4-fluoro-2-methylphenyl)-7-((2-iminooxazol-3(2*H*)-yl)methyl)-3,4-dihydroisoquinolin-1(2*H*)-one (19).

General procedure F was followed using **52** (30 mg, 0.06 mmol) and oxazol-2-amine (15 mg, 0.18 mmol) to obtain the title compound (19 mg, 63% yield). ¹H NMR (400 MHz, CDCl₃) δ 8.09 (d, *J*= 1.9 Hz, 1H), 7.24 (d, *J*= 1.9 Hz, 1H), 7.01 (dd, *J*= 8.6, 6.0 Hz, 1H), 6.96 (dd, *J*= 9.7, 2.6 Hz, 1H), 6.90 (td, *J*= 8.4, 2.6 Hz, 1H), 6.62 (d, *J*= 1.9 Hz, 1H), 6.46 (d, *J*= 2.3 Hz, 2H), 6.37 – 6.34 (m, 2H), 4.77 (s, 2H), 4.71 (ABq, *J*_{AB} = 14.8 Hz, 2H), 3.76 (s, 6H), 3.37 (d, *J*= 6.6 Hz, 2H), 2.65 – 2.57 (m, 1H), 2.55 – 2.47 (m, 1H), 2.01 (s, 3H); ¹³C NMR (100 MHz, CDCl₃) δ 164.3, 162.4 (d, *J*= 244.1 Hz), 161.2, 158.9, 139.7 (d, *J*= 7.2 Hz), 138.4 (d, *J*= 7.9 Hz), 136.3, 135.0, 132.4, 130.9 (d, *J*= 8.3 Hz), 130.4, 127.8, 127.0, 116.8 (d, *J*= 21.0 Hz), 116.2, 112.8 (d, *J*= 21.0 Hz), 106.2, 99.4, 55.5, 50.7, 47.9, 45.1, 25.7, 20.2; LCMS (ESI): >95%, *m/z* = 502.0 [M + H]⁺.

2-(3,5-Dimethoxybenzyl)-5-(4-fluoro-2-methylphenyl)-7-((2-iminothiazolidin-3-yl)methyl)-3,4-dihydroisoquinolin-1(2*H*)-one (20).

General procedure F was followed using **52** (35 mg, 0.07 mmol) and thiazolidin-2-imine (35.9 mg, 0.35 mmol) to obtain the title compound (22 mg, 60% yield). ¹H NMR (400 MHz, CDCl₃) δ 8.08 (s, 1H), 7.28 (s, 1H), 6.97 (m, 3H), 6.47 (d, *J*= 2.0 Hz, 2H), 6.37 (m, 1H), 4.72 (ABq, *J*_{AB} = 14.8 Hz, 2H), 4.66 (s, 2H), 3.77 (s, 6H), 3.57 (t, *J*= 6.8 Hz, 2H), 3.38 (t, *J*= 6.8 Hz, 2H), 3.16 (t, *J*= 6.8 Hz, 2H), 2.56 (m, 2H), 2.03 (s, 3H); ¹³C NMR (100 MHz, CDCl₃) δ 164.6, 162.4 (d, *J*= 244.0 Hz), 161.2, 139.8, 139.6, 138.5 (d, *J*= 7.0 Hz), 136.1, 135.7, 135.3, 132.7, 131.0 (d, *J*= 8.0 Hz), 130.2, 127.3, 116.8 (d, *J*= 21.0 Hz), 112.8 (d, *J*= 21.0 Hz), 106.3, 99.4, 55.5, 51.7, 50.7, 49.2, 45.2, 27.2, 25.7, 20.3; LCMS (ESI): >95%, *m/z* = 520.4 [M+H]⁺.

2-(3,5-Dimethoxybenzyl)-5-(4-fluoro-2-methylphenyl)-7-((2-iminopyrrolidin-1-yl)methyl)-3,4-dihydroisoquinolin-1(2*H*)-one (21).

General procedure F was followed using **52** (35 mg, 0.07 mmol) and pyrrolidin-2-imine hydrochloride (17 mg, 0.14 mmol) to obtain the title compound (21 mg, 60% yield). ¹H NMR (400 MHz, CDCl₃) δ 8.05 (s, 1H), 7.21 (s, 1H), 7.02 (dd, *J*= 6.0, 8.4 Hz, 1H), 6.92 (m, 2H), 6.47 (d, *J*= 2.0 Hz, 2H), 6.36 (m, 1H), 4.71 (ABq, *J*_{AB} = 14.8 Hz, 2H), 4.62 (s,

2H), 3.77 (s, 6H), 3.35 (m, 4H), 2.58 (m, 4H), 2.05 (s, 3H), 1.97 (m, 2H); ^{13}C NMR (100 MHz, CDCl_3) δ 169.2, 164.6, 162.4 (d, $J = 244.0$ Hz), 161.2, 139.8, 139.5, 138.5 (d, $J = 8.0$ Hz), 136.1, 135.6, 135.4 (d, $J = 3.0$ Hz), 132.5, 131.1 (d, $J = 8.0$ Hz), 130.2, 127.1, 116.8 (d, $J = 21.0$ Hz), 112.8 (d, $J = 21.0$ Hz), 106.2, 99.4, 55.5, 50.7, 50.1, 47.6, 45.2, 32.8, 25.7, 20.3, 19.7; LCMS (ESI): >95%, $m/z = 502.5$ [M+H] $^+$.

2-(3,5-Dimethoxybenzyl)-5-(4-fluoro-2-methylphenyl)-7-((5-imino-1-methyl-1,5-dihydro-4*H*-1,2,4-triazol-4-yl)methyl)-3,4-dihydroisoquinolin-1(2*H*)-one (22).

General procedure F was followed using **52** (30 mg, 0.06 mmol) and 1-methyl-1*H*-1,2,4-triazol-5-amine (18 mg, 0.18 mmol) to obtain the title compound (26 mg, 84% yield). ^1H NMR (400 MHz, CDCl_3) δ 8.10 (d, $J = 1.8$ Hz, 1H), 7.20 (d, $J = 1.9$ Hz, 1H), 7.18 (s, 1H), 7.00 (dd, $J = 8.5, 4.7$ Hz, 1H), 6.95 (dd, $J = 9.6, 4.1$ Hz, 1H), 6.90 (td, $J = 8.4, 3.9$ Hz, 1H), 6.45 (d, $J = 2.2$ Hz, 2H), 6.36 (t, $J = 2.2$ Hz, 1H), 4.83 (s, 2H), 4.70 (ABq, $J_{AB} = 14.7$ Hz, 2H), 3.75 (s, 6H), 3.40 (s, 3H), 3.37 (t, $J = 6.7$ Hz, 1H), 2.64 – 2.57 (m, 1H), 2.55 – 2.49 (m, 1H), 2.00 (s, 3H); ^{13}C NMR (100 MHz, CDCl_3) δ 164.2, 162.4 (d, $J = 244.1$ Hz), 161.2, 154.0, 140.0, 139.6, 138.4 (d, $J = 7.8$ Hz), 136.6, 135.0, 134.8 (d, $J = 3.0$ Hz), 134.0, 132.2, 130.0 (d, $J = 8.3$ Hz), 130.7, 127.1, 116.9 (d, $J = 21.1$ Hz), 112.9 (d, $J = 21.0$ Hz), 106.2, 99.4, 55.5, 50.7, 46.5, 45.1, 33.5, 25.7, 20.2; LCMS (ESI): >95%, $m/z = 516.0$ [M + H] $^+$.

Methyl 3-(hydroxymethyl)-5-(4,4,5,5-tetramethyl-1,3,2-dioxaborolan-2-yl)benzoate (24).

Bis(pinacolato)diboron (358 mg, 1.41 mmol), KOAc (276 mg, 2.82 mmol), and Pd(dppf)Cl₂ (69.0 mg, 0.094 mmol) were added to a solution of methyl 3-bromo-5-(hydroxymethyl)benzoate (**23**) (230 mg, 0.940 mmol) in 1,4-dioxane (9.4 mL). The reaction mixture was stirred at 85 °C overnight. The reaction mixture was concentrated and the residue was purified by flash column chromatography on silica gel (0 – 40% EtOAc:hexanes) to provide the title compound (264 mg, quantitative). ^1H NMR (400 MHz, CDCl_3) δ 8.39 (s, 1H), 8.15 (s, 1H), 7.99 (s, 1H), 4.75 (d, $J = 2.7$ Hz, 2H), 3.92 (s, 3H), 1.35 (s, 12H); ^{13}C NMR (100 MHz, CDCl_3) δ 167.2, 140.7, 137.8, 135.7, 130.9, 130.1, 127.9, 84.3, 64.9, 52.2, 25.0; LCMS (ESI): $m/z = 293.4$ [M + H] $^+$.

Methyl 4'-fluoro-5-(hydroxymethyl)-2'-methyl-[1,1'-biphenyl]-3-carboxylate (25).

To **24** (5.00 g, 30.3 mmol) in 1,4-dioxane:H₂O (3:1, 120 mL) was added 2-bromo-5-fluorotoluene (8.54 g, 45.4 mmol), K₂CO₃ (12.6 g, 90.9 mmol) and Pd(dppf)Cl₂ (1.11 g, 1.51 mmol). The mixture was degassed and then heated to 95 °C for 2 h. The reaction was cooled to room temperature, filtered through a pad of celite and washed with EtOAc. The filtrate was diluted with water (40 mL) and the layers were separated. The aqueous layer was extracted with EtOAc (3 × 40 mL) and the combined organic layers were washed with brine, dried (MgSO₄), filtered and concentrated. The residue was purified by flash column chromatography on silica gel (0 – 30% EtOAc:hexanes) to provide the title compound (5.67 g, 68% yield). ^1H NMR (400 MHz, CDCl_3) δ 8.02 (s, 1H), 7.89 (t, $J = 1.2$ Hz, 1H), 7.49 (s, 1H), 7.18 (dd, $J = 8.4, 6.0$ Hz, 1H), 6.99 – 6.90 (m, 2H), 4.79 (s, 2H), 3.92 (s, 3H), 2.23 (s, 3H), 2.06 (bs, 1H); ^{13}C NMR (100 MHz, CDCl_3) δ 167.1, 162.4 (d, $J = 245.0$ Hz), 141.7, 141.5, 137.9 (d, $J = 8.0$ Hz), 136.8 (d, $J = 3.0$ Hz), 132.3, 131.3 (d, $J = 8.0$ Hz), 130.5, 129.7,

126.6, 117.2 (d, $J = 21.0$ Hz), 112.9 (d, $J = 21.0$ Hz), 64.8, 52.4, 20.7; LCMS (ESI): $m/z = 275.1$ [M + H]⁺.

4'-Fluoro-5-(hydroxymethyl)-2'-methyl-[1,1'-biphenyl]-3-carboxylic acid (26).

To **25** (4.67 g, 17.0 mmol) in THF (68 mL) was added LiOH (2 M, 17 mL). The reaction was stirred at room temperature overnight. The reaction was then diluted with water (15 mL) and washed with EtOAc (15 mL). The aqueous layer was then acidified to pH ~ 2 using 1 M HCl and then extracted with EtOAc (3 × 15 mL). The combined organic layers were washed with brine, dried (MgSO₄), filtered and concentrated to provide the title compound (4.18 g, 94% yield). ¹H NMR (400 MHz, DMSO-*d*₆) δ 7.93 (s, 1H), 7.70 (s, 1H), 7.49 (s, 1H), 7.27 (dd, $J = 8.4, 6.0$ Hz, 1H), 7.20 (dd, $J = 10.0, 2.4$ Hz, 1H), 7.12 – 7.07 (m, 1H), 5.36 (bs, 1H), 4.61 (s, 2H), 2.22 (s, 3H); ¹³C NMR (100 MHz, DMSO-*d*₆) δ 167.3, 161.5 (d, $J = 242.0$ Hz), 143.3, 140.3, 137.6 (d, $J = 8.0$ Hz), 136.9 (d, $J = 3.0$ Hz), 131.4, 131.3 (d, $J = 8.0$ Hz), 130.8, 128.1, 125.9, 116.9 (d, $J = 20.0$ Hz), 112.9 (d, $J = 20.0$ Hz), 62.3, 20.1; LCMS (ESI): $m/z = 261.1$ [M + H]⁺.

N-Benzyl-4'-fluoro-5-(hydroxymethyl)-2'-methyl-[1,1'-biphenyl]-3-carboxamide (27).

General procedure A was followed using **26** (50 mg, 0.19 mmol) and benzylamine (20 mg, 0.19 mmol) to obtain the title compound (51.2 mg, 76% yield). ¹H NMR (400 MHz, CDCl₃) δ 7.77 (s, 1H), 7.62 (s, 1H), 7.42 (s, 1H), 7.37–7.29 (m, 5H), 7.17 (dd, $J = 8.4, 6.0$ Hz, 1H), 6.99 – 6.90 (m, 2H), 6.42 (bs, 1H), 4.79 (s, 2H), 4.67 (d, $J = 5.6$ Hz, 2H), 2.23 (s, 3H), 1.92 (bs, 1H); ¹³C NMR (200 MHz, CDCl₃) δ 167.1, 161.6 (d, $J = 244.0$ Hz), 141.9, 141.5, 138.0, 137.8 (d, $J = 8.0$ Hz), 136.7 (d, $J = 3.0$ Hz), 134.8, 131.2 (d, $J = 8.0$ Hz), 130.8, 128.9, 128.0, 127.8, 127.1, 123.9, 117.0 (d, $J = 20.0$ Hz), 112.8 (d, $J = 20.0$ Hz), 64.7, 44.3, 20.6; LCMS (ESI): $m/z = 350.1$ [M + H]⁺.

4'-Fluoro-5-(hydroxymethyl)-2'-methyl-N-(3-methylbenzyl)-[1,1'-biphenyl]-3-carboxamide (28).

General procedure A was followed using **26** (50 mg, 0.19 mmol) and 3-methylbenzylamine (23 mg, 0.19 mmol) to obtain the title compound (58.6 mg, 84% yield). ¹H NMR (400 MHz, CDCl₃) δ 7.77 (s, 1H), 7.62 (s, 1H), 7.42 (s, 1H), 7.25 – 7.22 (m, 1H), 7.17 – 7.11 (m, 3H), 6.99 – 6.90 (m, 2H), 6.40 (bs, 1H), 4.79 (s, 2H), 4.62 (d, $J = 5.6$ Hz, 2H), 2.35 (s, 3H), 2.23 (s, 3H), 1.92 (bs, 1H); ¹³C NMR (100 MHz, CDCl₃) δ 166.9, 160.9 (d, $J = 244.0$ Hz), 141.8, 141.4, 138.5, 137.8, 137.7 (d, $J = 8.0$ Hz), 136.6 (d, $J = 3.0$ Hz), 134.7, 131.1 (d, $J = 8.0$ Hz), 130.6, 128.8, 128.7, 128.4, 127.0, 125.0, 123.8, 116.9 (d, $J = 21.0$ Hz), 112.7 (d, $J = 21.0$ Hz), 64.6, 44.2, 21.3, 20.5; LCMS (ESI): $m/z = 364.0$ [M + H]⁺.

N-(3-Chlorobenzyl)-4'-fluoro-5-(hydroxymethyl)-2'-methyl-[1,1'-biphenyl]-3-carboxamide (29).

General procedure A was followed using **26** (50 mg, 0.19 mmol) and 3-chlorobenzylamine (27 mg, 0.19 mmol) to obtain the title compound (60.3 mg, 82% yield). ¹H NMR (400 MHz, MeOD) δ 7.87 (s, 1H), 7.71 (s, 1H), 7.50 (s, 1H), 7.39 (s, 1H), 7.36 – 7.24 (m, 4H), 7.08 – 6.97 (m, 2H), 4.74 (s, 2H), 4.59 (s, 2H), 2.27 (s, 3H); ¹³C NMR (200 MHz, MeOD) δ 170.1, 163.8 (d, $J = 244.0$ Hz), 143.8, 143.1, 142.9, 139.4 (d, $J = 8.0$ Hz), 138.7 (d, $J = 3.0$ Hz),

135.7, 135.5, 132.5 (d, $J = 8.0$ Hz), 132.2, 131.2, 128.7, 128.4, 128.2, 127.0, 125.6, 117.9 (d, $J = 20.0$ Hz), 113.7 (d, $J = 20.0$ Hz), 64.8, 44.2, 20.8; LCMS (ESI): $m/z = 384.0$ [M + H]⁺.

***N*-(3-Methoxybenzyl)-4'-fluoro-5-(hydroxymethyl)-2'-methyl-[1,1'-biphenyl]-3-carboxamide (30).**

General procedure A was followed using **26** (101 mg, 0.39 mmol) and 3-methoxybenzylamine (53 mg, 0.39 mmol) to obtain the title compound (93 mg, 63% yield). ¹H NMR (400 MHz, CDCl₃) δ 7.75 (s, 1H), 7.61 (s, 1H), 7.41 (s, 1H), 7.28 – 7.24 (m, 1H), 7.16–7.12 (m, 1H), 6.98 – 6.91 (m, 4H), 6.84–6.82 (m, 1H), 6.51 – 6.48 (m, 1H), 4.76 (s, 2H), 4.60 (d, $J = 5.6$ Hz, 2H), 3.80 (s, 3H), 2.22 (s, 3H); ¹³C NMR (150 MHz, CDCl₃) δ 167.1, 162.2 (d, $J = 246.3$ Hz), 160.0, 141.8, 141.5, 139.6, 137.7 (d, $J = 8.1$ Hz), 136.7, (d, $J = 2.4$ Hz), 134.7, 131.1 (d, $J = 8.1$ Hz), 130.8, 129.9, 127.0, 123.8, 120.2, 116.9 (d, $J = 21.8$ Hz), 113.7, 113.0, 112.7 (d, $J = 21.8$ Hz), 66.5, 55.3, 44.2, 20.6; LCMS (ESI): $m/z = 380.4$ [M + H]⁺.

4'-Fluoro-5-(hydroxymethyl)-2'-methyl-*N*-(3-(trifluoromethoxy)benzyl)-[1,1'-biphenyl]-3-carboxamide (31).

General procedure A was followed using **26** (50 mg, 0.19 mmol) and 3-(trifluoromethoxy)benzylamine (37 mg, 0.19 mmol) to obtain the title compound (63.7 mg, 76% yield). ¹H NMR (400 MHz, MeOD) δ 7.87 (s, 1H), 7.71 (s, 1H), 7.50 (s, 1H), 7.47 – 7.43 (m, 1H), 7.39 – 7.37 (m, 1H), 7.29 (s, 1H), 7.27 – 7.23 (m, 1H), 7.19 (d, $J = 8.0$ Hz, 1H), 7.08 – 7.05 (m, 1H), 7.02–6.97 (m, 1H), 4.74 (s, 2H), 4.63 (s, 2H), 2.27 (s, 3H); ¹³C NMR (200 MHz, MeOD) δ 170.1, 163.8 (d, $J = 244.0$ Hz), 150.9, 143.9, 143.3, 143.1, 139.3 (d, $J = 8.0$ Hz), 138.7 (d, $J = 3.0$ Hz), 135.7, 132.5 (d, $J = 8.0$ Hz), 132.2, 131.4, 128.2, 127.4, 125.6, 121.2, 120.7, 117.9 (d, $J = 20.0$ Hz), 113.7 (d, $J = 20.0$ Hz), 64.8, 44.1, 20.8; LCMS (ESI): $m/z = 433.9$ [M + H]⁺.

***N*-(3,4-Dichlorobenzyl)-4'-fluoro-5-(hydroxymethyl)-2'-methyl-[1,1'-biphenyl]-3-carboxamide (32).**

General Procedure A was followed using **26** (50 mg, 0.19 mmol) and 3,4-dichlorobenzylamine (34 mg, 0.19 mmol) to obtain the title compound (67.1 mg, 84% yield). ¹H NMR (400 MHz, DMSO-*d*₆) δ 7.89 (s, 1H), 7.72 (s, 1H), 7.59 (s, 1H), 7.57 (s, 1H), 7.44 (s, 1H), 7.33 – 7.25 (m, 2H), 7.19 – 7.07 (m, 2H), 4.63 (d, $J = 5.6$ Hz, 2H), 4.48 (d, $J = 5.6$ Hz, 2H), 2.24 (s, 3H); ¹³C NMR (100 MHz, DMSO-*d*₆) δ 166.6, 163.0 (d, $J = 243.0$ Hz), 143.4, 141.3, 140.5, 138.1 (d, $J = 8.0$ Hz), 137.6 (d, $J = 3.0$ Hz), 134.3, 131.8 (d, $J = 8.0$ Hz), 131.2, 130.9, 130.3, 129.7, 129.6, 128.1, 126.5, 124.7, 117.2 (d, $J = 21.0$ Hz), 113.1 (d, $J = 21.0$ Hz), 63.0, 42.2, 20.6; LCMS (ESI): $m/z = 417.9$ [M + H]⁺.

***N*-(4-Chloro-3-methylbenzyl)-4'-fluoro-5-(hydroxymethyl)-2'-methyl-[1,1'-biphenyl]-3-carboxamide (33).**

General procedure A was followed using **26** (50 mg, 0.19 mmol) and 4-chloro-3-methylbenzylamine (30 mg, 0.19 mmol) to obtain the title compound (61.1 mg, 80% yield). ¹H NMR (400 MHz, DMSO-*d*₆) δ 7.88 (s, 1H), 7.71 (s, 1H), 7.42 (s, 1H), 7.36 (d, $J = 8.4$ Hz, 1H), 7.29 – 7.25 (m, 2H), 7.20 – 7.16 (m, 2H), 7.13 – 7.08 (m, 1H), 4.61 (d, $J = 5.6$ Hz,

2H), 4.44 (d, $J = 5.6$ Hz, 2H), 2.30 (s, 3H), 2.24 (s, 3H); ^{13}C NMR (100 MHz, DMSO- d_6) δ 166.4, 161.8 (d, $J = 242.0$ Hz), 143.4, 140.5, 139.1, 138.1 (d, $J = 8.0$ Hz), 137.6 (d, $J = 3.0$ Hz), 135.5, 134.5, 131.8 (d, $J = 8.0$ Hz), 130.6, 130.2, 129.1, 127.0, 126.4, 124.7, 117.2 (d, $J = 20.0$ Hz), 113.1 (d, $J = 20.0$ Hz), 63.0, 42.5, 20.6, 20.0; LCMS (ESI): $m/z = 397.9$ [M + H]⁺.

***N*-(4-Fluoro-3-methylbenzyl)-4'-fluoro-5-(hydroxymethyl)-2'-methyl-[1,1'-biphenyl]-3-carboxamide (34).**

General procedure A was followed using **26** (75 mg, 0.29 mmol) and 4-fluoro-3-methylbenzylamine (40 mg, 0.29 mmol) to obtain the title compound (92 mg, 84% yield). ^1H NMR (400 MHz, DMSO- d_6) δ 9.06 (t, $J = 5.9$ Hz, 1H), 7.87 (s, 1H), 7.71 (s, 1H), 7.42 (s, 1H), 7.29–7.06 (series of m, 6H), 5.33 (t, $J = 5.7$ Hz, 1H), 4.61 (d, $J = 5.9$ Hz, 2H), 4.43 (d, $J = 5.7$ Hz, 2H), 2.24 (s, 3H), 2.22 (s, 3H); ^{13}C NMR (150 MHz, DMSO- d_6) δ 166.4, 161.9 (d, $J = 242.0$ Hz), 160.1 (d, $J = 240.0$ Hz), 159.3, 143.4, 140.5, 138.1 (d, $J = 8.0$ Hz), 137.7 (d, $J = 2.5$ Hz), 136.0 (d, $J = 3.0$ Hz), 134.6, 131.8 (d, $J = 8.4$ Hz), 131.0 (d, $J = 5.1$ Hz), 130.2, 127.0 (d, $J = 8.4$ Hz), 126.5, 124.7, 124.3 (d, $J = 17.1$ Hz), 117.2 (d, $J = 20.9$ Hz), 115.1 (d, $J = 22.0$ Hz), 113.1 (d, $J = 20.8$ Hz), 63.0, 42.5, 20.7, 14.6; LCMS (ESI): $m/z = 382.3$ [M + H]⁺.

***N*-(4-Fluoro-3-methoxybenzyl)-4'-fluoro-5-(hydroxymethyl)-2'-methyl-[1,1'-biphenyl]-3-carboxamide (35).**

General procedure A was followed using **26** (76 mg, 0.29 mmol) and 4-fluoro-3-methoxybenzylamine (45 mg, 0.29 mmol) to obtain the title compound (43 mg, 37% yield). ^1H NMR (400 MHz, DMSO- d_6) δ 9.05 (t, $J = 6.0$ Hz, 1H), 7.86 (s, 1H), 7.70 (s, 1H), 7.41 (s, 1H), 7.28–7.25 (m, 1H), 7.20–7.08 (series of m, 4H), 6.88–6.85 (m, 1H), 5.32 (t, $J = 5.7$ Hz, 1H), 4.59 (d, $J = 5.7$ Hz, 2H), 4.44 (d, $J = 6.0$ Hz, 2H), 3.81 (s, 3H), 2.22 (s, 3H); ^{13}C NMR (150 MHz, DMSO- d_6) δ 166.5, 161.9 (d, $J = 242.3$ Hz), 151.0 (d, $J = 240.8$ Hz), 147.3 (d, $J = 10.7$ Hz), 143.5, 140.5, 138.2 (d, $J = 8.1$ Hz), 137.7 (d, $J = 2.3$ Hz), 137.0 (d, $J = 3.3$ Hz), 135.7, 131.9 (d, $J = 8.2$ Hz), 130.3, 126.5, 124.8, 120.0 (d, $J = 6.7$ Hz), 117.2 (d, $J = 20.9$ Hz), 116.0 (d, $J = 18.03$ Hz), 113.5, 113.1 (d, $J = 20.7$ Hz), 63.0, 56.3, 42.8, 20.7; LCMS (ESI): $m/z = 398.3$ [M + H]⁺.

***N*-(3,5-Dimethylbenzyl)-4'-fluoro-5-(hydroxymethyl)-2'-methyl-[1,1'-biphenyl]-3-carboxamide (36)**

General procedure A was followed using **26** (75 mg, 0.29 mmol) and 3,5-dimethylbenzylamine (39 mg, 0.29 mmol) to obtain the title compound (87 mg, 80% yield). ^1H NMR (400 MHz, DMSO- d_6) δ 9.01 (t, $J = 5.7$ Hz, 1H), 7.88 (s, 1H), 7.72 (s, 1H), 7.42 (s, 1H), 7.29–7.26 (m, 1H), 7.19 (dd, $J = 10.1, 2.7$ Hz, 1H), 7.11 (dt, $J = 8.8, 2.9$ Hz, 1H), 6.92 (s, 2H), 6.87 (s, 1H), 5.33 (t, $J = 5.7$ Hz, 1H), 4.60 (d, $J = 5.7$ Hz, 2H), 4.41 (d, $J = 5.9$ Hz, 2H), 2.24 (s, 3H); ^{13}C NMR (150 MHz, DMSO- d_6) δ 166.3, 161.9 (d, $J = 242.1$ Hz), 143.4, 140.5, 140.0, 138.1 (d, $J = 7.9$ Hz), 137.7 (d, $J = 2.4$ Hz), 137.6, 134.7, 131.8 (d, $J = 8.3$ Hz), 130.2, 128.6, 126.5, 125.6, 124.8, 117.2 (d, $J = 20.9$ Hz), 113.1 (d, $J = 20.8$ Hz), 63.0, 43.1, 21.4, 20.7; LCMS (ESI): $m/z = 378.4$ [M + H]⁺.

***N*-(3,5-Dichlorobenzyl)-4'-fluoro-5-(hydroxymethyl)-2'-methyl-[1,1'-biphenyl]-3-carboxamide (37).**

General procedure A was followed using **26** (68 mg, 0.26 mmol) and 3,5-dichlorobenzylamine (46 mg, 0.26 mmol) to obtain the title compound (87 mg, 80% yield). ¹H NMR (400 MHz, DMSO-*d*₆) δ 9.14 (t, *J* = 5.8 Hz, 1H), 7.89 (s, 1H), 7.72 (s, 1H), 7.49 (t, *J* = 1.9 Hz, 1H), 7.44 (s, 1H), 7.38 (d, *J* = 1.9 Hz, 2H), 7.30 – 7.26 (m, 1H), 7.20 (dd, *J* = 7.5, 2.8 Hz, 1H), 7.12 (dt, *J* = 8.5, 2.7 Hz, 1H), 5.34 (t, *J* = 5.9 Hz, 1H), 4.61 (d, *J* = 5.8 Hz, 2H), 4.48 (d, *J* = 5.9 Hz, 2H), 2.25 (s, 3H); ¹³C NMR (150 MHz, DMSO-*d*₆) δ 166.7, 161.9 (d, *J* = 242.3 Hz), 144.6, 143.6, 140.6, 138.2 (d, *J* = 8.1 Hz), 137.6 (d, *J* = 2.7 Hz), 134.4, 134.2, 131.8 (d, *J* = 8.5 Hz), 130.5, 126.9, 126.6, 126.5, 124.7, 117.2 (d, *J* = 20.9 Hz), 113.2 (d, *J* = 20.9 Hz), 63.0, 42.4, 20.7; LCMS (ESI): *m/z* = 418.3 [M + H]⁺.

***N*-(3,5-Dimethoxybenzyl)-4'-fluoro-5-(hydroxymethyl)-2'-methyl-[1,1'-biphenyl]-3-carboxamide (38).**

General procedure A was followed using **26** (100 mg, 0.38 mmol) and 3,5-dimethoxybenzylamine (64 mg, 0.38 mmol) to obtain the title compound (93 mg, 59% yield). ¹H NMR (400 MHz, CDCl₃) δ 7.76 (s, 1H), 7.61 (s, 1H), 7.41 (s, 1H), 7.17 – 7.13 (m, 1H), 6.98 – 6.89 (m, 2H), 6.49 (d, *J* = 2.3 Hz, 2H), 6.38 (t, *J* = 2.2 Hz, 1H), 4.77 (s, 2H), 4.57 (d, *J* = 5.8 Hz, 2H), 3.77 (s, 6H), 2.22 (s, 3H); ¹³C NMR (150 MHz, CDCl₃) δ 167.1, 162.2 (d, *J* = 244.7 Hz), 161.2, 141.9, 141.5, 140.3, 137.7 (d, *J* = 7.7 Hz), 136.7 (d, *J* = 2.7 Hz), 134.7, 131.1 (d, *J* = 7.7 Hz), 13.8, 127.1, 123.9, 116.9 (d, *J* = 21.2 Hz), 112.7 (d, *J* = 21.2 Hz), 106.0, 99.5, 64.7, 55.4, 44.4, 20.6; LCMS (ESI): *m/z* = 410.4 [M + H]⁺.

Methyl 2-(2,4-dimethoxybenzyl)-5-hydroxy-1-oxo-1,2,3,4-tetrahydroisoquinoline-7-carboxylate (40).

To a solution of dimethyl 2-hydroxy-2,3-dihydrobenzofuran-4,6-dicarboxylate (**39**) (518.7 mg, 2.05 mmol, 1 equiv.) in CH₂Cl₂ (40 mL) was added 2,4-dimethoxy benzylamine (515.8 mg, 3.08 mmol, 1.5 equiv.). The reaction was stirred at room temperature for 10 min, then NaBH(OAc)₃ (653.8 mg, 3.08 mmol, 1.5 equiv) was added. The resulting mixture was stirred at room temperature for 16 h and followed by LC-MS analysis. The solvent was removed under reduced pressure and toluene (8 mL) was added to the residue. The mixture was heated at 110 °C for 1 h, then cooled to room temperature. The mixture was extracted with EtOAc and water. The organic layer was dried (Na₂SO₄) and concentrated. The residue was purified by silica gel column chromatography (0 – 70% EtOAc:hexanes) to provide **40** (503.0 mg, 65% yield) as a white foam. ¹H NMR (400 MHz, CDCl₃) δ 8.37 (s, 1H), 7.67 (s, 1H), 7.29 (s, 1H), 6.44 (m, 2H), 4.75 (s, 2H), 3.88 (s, 3H), 3.84 (s, 3H), 3.82 (s, 3H), 3.54 (t, *J* = 6.8 Hz, 2H), 2.96 (t, *J* = 6.8 Hz, 2H); ¹³C NMR (100 MHz, CDCl₃) δ 167.0, 164.3, 160.5, 158.80, 152.8, 131.1, 130.9, 130.7, 129.3, 121.6, 118.8, 117.6, 104.4, 98.5, 55.5, 52.3, 45.4, 45.2, 21.9; LCMS (ESI): *m/z* = 372.4 [M + H]⁺.

Methyl 2-(2,4-dimethoxybenzyl)-1-oxo-5-(((trifluoromethyl)sulfonyl)oxy)-1,2,3,4-tetrahydroisoquinoline-7-carboxylate (41).

To a solution of **40** (2.1 g, 5.65 mmol, equiv.) in CH₂Cl₂ (25 mL) was added *N,N*-diisopropylethylamine (1.48 mL, 8.5 mmol, 1.5 equiv.), *N*-Phenyl-

bis(trifluoromethanesulfonimide) (2.42 g, 6.78 mmol, 1.2 equiv.). The reaction mixture was stirred at room temperature for 16 h, then diluted with CH₂Cl₂ and washed with water. The organic layer was dried (Na₂SO₄) and concentrated. The residue was purified by silica gel column chromatography (0 – 50% EtOAc:hexanes) to provide **41** (2.2 g, 75% yield) as a light yellow solid. ¹H NMR (400 MHz, CDCl₃) δ 8.82 (s, 1H), 8.02 (s, 1H), 7.30 (m, 1H), 6.48 (m, 2H), 4.75 (s, 2H), 3.96 (s, 3H), 3.84 (s, 3H), 3.81 (s, 3H), 3.60 (t, *J* = 6.4 Hz, 2H), 3.05 (t, *J* = 6.4 Hz, 2H); ¹³C NMR (100 MHz, CDCl₃) δ 165.0, 162.1, 160.8, 158.9, 145.9, 136.2, 133.0, 131.5, 131.05, 129.6, 125.1, 118.8 (q, *J* = 318.0 Hz), 117.3, 104.6, 98.7, 55.6, 52.9, 45.5, 44.6, 23.2; LCMS (ESI): *m/z* = 504.4 [M + H]⁺.

Methyl 1-oxo-5-(((trifluoromethyl)sulfonyl)oxy)-1,2,3,4-tetrahydroisoquinoline-7-carboxylate (42).

To a solution of **41** (1.8 g, 3.6 mmol, 1 equiv.) in CH₂Cl₂ (10 mL) was added anisole (1.96 mL, 18 mmol, 5 equiv.) and TFA (20 mL). The reaction was stirred at room temperature overnight. The solvent was removed under reduced pressure. The residue was dissolved in EtOAc, and washed with sat. NaHCO₃. The organic layer was dried (Na₂SO₄) and concentrated. The residue was purified by silica gel column chromatography (0 – 50% EtOAc:hexanes) to provide **42** (1.0 g, 78% yield) as a white solid. ¹H NMR (400 MHz, CDCl₃) δ 8.77 (s, 1H), 8.09 (s, 1H), 6.74 (brs, 1H), 3.97 (s, 3H), 3.65 (m, 2H), 3.16 (t, *J* = 6.4 Hz, 2H); ¹³C NMR (100 MHz, CDCl₃) δ 164.8, 163.7, 146.2, 136.8, 132.1, 131.2, 129.3, 125.9, 118.7 (q, *J* = 319.0 Hz), 53.0, 39.4, 23.4; LCMS (ESI): *m/z* = 354.2 [M + H]⁺.

Methyl 5-(4-fluoro-2-methylphenyl)-1-oxo-1,2,3,4-tetrahydroisoquinoline-7-carboxylate (43).

To a solution of **42** (2.53 g, 7.16 mmol, 1 equiv.) in 1,4-dioxane (72 mL) was added (4-fluoro-2-methylphenyl) boronic acid (1.43 g, 9.31 mmol, 1.3 equiv.), Na₂CO₃ (1.9 g, 17.9 mmol, 2.5 equiv.), water (7.2 mL), and Pd(PPh₃)₄ (497 mg, 0.43 mmol, 0.06 equiv.). The mixture was degassed and back filled with Argon gas, then heated at 80 °C for 16 h. The mixture was diluted with EtOAc, and washed with water. The organic layer was dried (Na₂SO₄) and concentrated. The residue was purified by silica gel column chromatography (0 – 80% EtOAc:hexanes) to provide **43** (2.1 g, 93% yield) as an off-white foam. ¹H NMR δ 8.78 (s, 1H), 7.99 (s, 1H), 7.00 (m, 3H), 6.21 (brs, 1H), 3.94 (s, 3H), 3.50 (m, 2H), 2.69 (m, 2H), 2.05 (s, 3H); ¹³C NMR (100 MHz, CDCl₃) δ 166.4, 165.7, 162.5 (d, *J* = 245.0 Hz), 142.1, 139.8, 138.4 (d, *J* = 8.0 Hz), 134.6 (d, *J* = 5.0 Hz), 134.2, 130.9 (d, *J* = 8.0 Hz), 129.9, 129.1, 128.7, 117.0 (d, *J* = 21.0 Hz), 113.04 (d, *J* = 21.0 Hz), 52.4, 39.8, 26.3, 20.1; LCMS (ESI): *m/z* = 314.4 [M + H]⁺.

Methyl 2-(4-chloro-3-methylbenzyl)-5-(4-fluoro-2-methylphenyl)-1-oxo-1,2,3,4-tetrahydroisoquinoline-7-carboxylate (44).

General procedure C was followed using **43** (316 mg, 1.0 mmol) and 1-chloro-4-(chloromethyl)-2-methylbenzene (230 mg, 1.3 mmol) to obtain the title compound (260.0 mg, 57% yield). ¹H NMR (400 MHz, CDCl₃) δ 8.84 (d, *J* = 1.6 Hz, 1H), 7.97 (d, *J* = 1.6 Hz, 1H), 7.28 (d, *J* = 8.4 Hz, 1H), 7.20 (s, 1H), 7.10 (m, 1H), 6.99 (m, 4H), 4.73 (ABq, *J*_{AB} = 14.8 Hz, 2H), 3.95 (s, 3H), 3.39 (t, *J* = 6.4 Hz, 2H), 2.64 (m, 2H), 2.35 (s, 3H), 2.03 (s, 3H); ¹³C NMR (100 MHz, CDCl₃) δ 166.6, 163.9, 162.6 (d, *J* = 245.0 Hz), 141.3, 139.5, 138.5

(d, $J = 7.0$ Hz), 136.6, 135.8, 134.5, 133.9, 133.8, 131.1 (d, $J = 5.0$ Hz), 131.0, 130.3, 129.5, 129.3, 127.1, 117.0 (d, $J = 22.0$ Hz), 113.0 (d, $J = 22.0$ Hz), 52.5, 50.2, 45.0, 26.2, 20.2; LCMS (ESI): $m/z = 452.4$ [M + H]⁺.

Methyl 5-(4-fluoro-2-methylphenyl)-2-(4-fluoro-3-methylbenzyl)-1-oxo-1,2,3,4-tetrahydroisoquinoline-7-carboxylate (45).

General procedure C was followed using **43** (219 mg, 0.70 mmol) and 4-(bromomethyl)-1-fluoro-2-methylbenzene (284 mg, 1.4 mmol) to obtain the title compound (357.0 mg, quant.). ¹H NMR (400 MHz, CDCl₃) δ 8.81 (d, $J = 1.4$ Hz, 1H), 8.00 (s, 1H), 7.93 (d, $J = 1.5$ Hz, 1H), 7.14 (d, $J = 7.2$ Hz, 1H), 7.11 – 7.08 (m, 1H), 7.02 – 6.88 (m, 3H), 4.70 (ABq, $J_{AB} = 14.6$ Hz, 2H), 3.91 (s, 3H), 3.37 (t, $J = 6.6$ Hz, 2H), 2.69 – 2.52 (m, 2H), 2.22 (s, 3H), 2.01 (s, 3H); ¹³C NMR (100 MHz, CDCl₃) δ 166.5, 163.8, 162.6, 162.5 (d, $J = 245.3$ Hz), 160.9 (d, $J = 243.2$ Hz), 141.3, 139.5, 138.4 (d, $J = 8.0$ Hz), 134.5 (d, $J = 3.1$ Hz), 133.8, 132.6 (d, $J = 3.5$ Hz), 131.5 (d, $J = 5.1$ Hz), 130.9 (d, $J = 8.3$ Hz), 130.3, 129.2 (d, $J = 2.3$ Hz), 127.2 (d, $J = 8.0$ Hz), 125.3 (d, $J = 17.6$ Hz), 116.9 (d, $J = 21.2$ Hz), 115.2 (d, $J = 22.5$ Hz), 112.9 (d, $J = 21.3$ Hz), 52.4, 50.0, 44.8, 36.6, 31.5, 26.1, 20.1, 14.6 (d, $J = 3.4$ Hz); LCMS (ESI): $m/z = 436.0$ [M + H]⁺.

Methyl 2-(3,5-dimethoxybenzyl)-5-(4-fluoro-2-methylphenyl)-1-oxo-1,2,3,4-tetrahydroisoquinoline-7-carboxylate (46).

General procedure C was followed using **43** (0.68 g, 2.1 mmol) and 3,5-dimethoxybenzyl bromide (0.64 g, 2.8 mmol) to obtain the title compound (0.77 g, 78% yield). ¹H NMR (400 MHz, CDCl₃) δ 8.84 (d, $J = 1.6$ Hz, 1H), 7.96 (d, $J = 1.6$ Hz, 1H), 7.00 (m, 3H), 6.48 (m, 2H), 6.37 (m, 1H), 4.74 (ABq, $J_{AB} = 14.8$ Hz, 2H), 3.94 (s, 3H), 3.76 (s, 6H), 3.40 (t, $J = 6.4$ Hz, 2H), 2.63 (m, 2H), 2.05 (s, 3H); ¹³C NMR (100 MHz, CDCl₃) δ 166.5, 163.8, 162.5 (d, $J = 246.0$ Hz), 161.2, 141.3, 139.5, 139.4, 138.4 (d, $J = 8.0$ Hz), 134.5 (d, $J = 3.0$ Hz), 133.8, 130.9 (d, $J = 8.0$ Hz), 130.3, 129.2, 116.9 (d, $J = 21.0$ Hz), 112.9 (d, $J = 21.0$ Hz), 106.3, 99.4, 55.5, 52.4, 50.7, 44.8, 26.1, 20.2; LCMS (ESI): $m/z = 464.4$ [M + H]⁺.

2-(4-Chloro-3-methylbenzyl)-5-(4-fluoro-2-methylphenyl)-7-(hydroxymethyl)-3,4-dihydroisoquinolin-1(2H)-one (47).

General procedure D was followed using **44** (263 mg, 0.58 mmol) to obtain the title compound (168.0 mg, 68% yield). ¹H NMR (400 MHz, CDCl₃) δ 8.19 (s, 1H), 7.32 (s, 1H), 7.25 (d, $J = 8.0$ Hz, 1H), 7.18 (s, 1H), 7.07 (m, 1H), 7.01 (dd, $J = 6.0, 8.4$ Hz, 1H), 6.89 (dt, $J = 2.4, 8.4$ Hz, 1H), 4.75 (s, 2H), 4.70 (ABq, $J_{AB} = 14.8$ Hz, 2H), 3.35 (t, $J = 6.4$ Hz, 2H), 3.18 (brs, 1H), 2.55 (m, 2H), 2.33 (s, 3H), 2.02 (s, 3H); ¹³C NMR (100 MHz, CDCl₃) δ 164.9, 162.3 (d, $J = 245.0$ Hz), 140.2, 139.2, 138.4 (d, $J = 8.0$ Hz), 136.4, 135.9, 135.5, 135.4 (d, $J = 3.0$ Hz), 133.6, 131.8, 131.0 (d, $J = 8.0$ Hz), 130.8, 129.8, 129.3, 126.9, 126.4, 116.7 (d, $J = 21.0$ Hz), 112.7 (d, $J = 21.0$ Hz), 64.6, 50.1, 45.3, 25.6, 20.2; LCMS (ESI): $m/z = 424.4$ [M + H]⁺.

5-(4-Fluoro-2-methylphenyl)-2-(4-fluoro-3-methylbenzyl)-7-(hydroxymethyl)-3,4-dihydroisoquinolin-1(2H)-one (48).

General procedure D was followed using **45** (327 mg, 0.7 mmol) to obtain the title compound (306 mg, quant.). ¹H NMR (400 MHz, CDCl₃) δ 8.16 (s, 1H), 7.31 (s, 1H), 7.15 (d, *J* = 7.3 Hz, 1H), 7.11 – 7.08 (m, 1H), 7.04 – 7.01 (m, 1H), 6.97 – 6.89 (m, 3H), 5.00 (brs, 1H), 4.70 (ABq, *J*_{AB} = 14.7 Hz, 2H), 3.91 – 3.72 (m, 2H), 3.35 (t, *J* = 6.5 Hz, 2H), 2.62 – 2.49 (m, 2H), 2.24 (s, 3H), 2.03 (s, 3H); ¹³C NMR (100 MHz, CDCl₃) δ 164.7, 162.3 (d, *J* = 244.0 Hz), 160.9 (d, *J* = 243.0 Hz), 138.5 (d, *J* = 8.8 Hz), 135.5, 132.9, 131.4 (d, *J* = 5.2 Hz), 131.0 (d, *J* = 8.2 Hz), 129.9, 127.2 (d, *J* = 8.1 Hz), 126.3, 126.1, 125.3, 125.2, 116.8 (d, *J* = 21.2 Hz), 115.2 (d, *J* = 22.5 Hz), 112.8 (d, *J* = 20.8 Hz), 50.0, 45.3, 37.1, 25.7, 20.2, 14.7 (d, *J* = 3.4 Hz); LCMS (ESI): *m/z* = 408.0 [M + H]⁺.

2-(3,5-Dimethoxybenzyl)-5-(4-fluoro-2-methylphenyl)-7-(hydroxymethyl)-3,4-dihydroisoquinolin-1(2H)-one (49).

General procedure D was followed using **46** (0.77 g, 1.7 mmol) to obtain the title compound (0.60 g, 83% yield). ¹H NMR (400 MHz, CDCl₃) δ 8.18 (d, *J* = 1.6 Hz, 1H), 7.32 (d, *J* = 1.6 Hz, 1H), 7.03 (dd, *J* = 6.0, 8.4 Hz, 1H), 6.97 (dd, *J* = 2.8, 10.0 Hz, 1H), 6.91 (m, 1H), 6.47 (d, *J* = 2.0 Hz, 2H), 6.36 (m, 1H), 4.73 (m, 4H), 3.76 (s, 6H), 3.38 (t, *J* = 6.4 Hz, 2H), 2.58 (m, 2H), 2.15 (m, 1H), 2.04 (s, 3H); ¹³C NMR (100 MHz, CDCl₃) δ 164.8, 162.4 (d, *J* = 245.0 Hz), 161.2, 139.9, 139.8, 139.3, 138.5 (d, *J* = 7.0 Hz), 135.7, 135.4 (d, *J* = 3.0 Hz), 131.7, 131.0 (d, *J* = 9.0 Hz), 130.1, 126.4, 116.8 (d, *J* = 21.0 Hz), 112.8 (d, *J* = 21.0 Hz), 106.2, 99.5, 64.9, 55.5, 50.7, 45.3, 25.7, 20.2; LCMS (ESI): *m/z* = 436.4 [M + H]⁺.

7-(Bromomethyl)-2-(4-chloro-3-methylbenzyl)-5-(4-fluoro-2-methylphenyl)-3,4-dihydroisoquinolin-1(2H)-one (50).

General procedure E was followed using **47** (90 mg, 0.21 mmol) to obtain the title compound (94.0 mg, 91% yield). ¹H NMR (400 MHz, CDCl₃) δ 8.19 (d, *J* = 1.6 Hz, 1H), 7.31 (d, *J* = 1.6 Hz, 1H), 7.24 (s, 1H), 7.17 (s, 1H), 7.03 (m, 4H), 6.94 (m, 2H), 4.69 (ABq, *J*_{AB} = 14.8 Hz, 2H), 4.52 (s, 3H), 3.34 (t, *J* = 6.4 Hz, 2H), 2.53 (m, 2H), 2.33 (s, 3H), 2.02 (s, 3H); ¹³C NMR (100 MHz, CDCl₃) δ 164.2, 162.5 (d, *J* = 245.0 Hz), 139.8, 138.5 (d, *J* = 8.0 Hz), 136.8, 136.7, 136.6, 135.9, 134.9 (d, *J* = 3.0 Hz), 133.7, 131.0, 130.9, 130.4, 129.4, 128.4, 127.0, 116.9 (d, *J* = 21.0 Hz), 113.0 (d, *J* = 21.0 Hz), 50.1, 45.2, 32.7, 25.8, 20.2; LCMS (ESI): *m/z* = 486.4 [M + H]⁺.

7-(Bromomethyl)-5-(4-fluoro-2-methylphenyl)-2-(4-fluoro-3-methylbenzyl)-3,4-dihydroisoquinolin-1(2H)-one (51).

General procedure E was followed using **48** (320 mg, 0.78 mmol) to obtain the title compound (197.8 mg, 54% yield). ¹H NMR (400 MHz, CDCl₃) δ 8.21 (d, *J* = 1.6 Hz, 1H), 7.32 (d, *J* = 1.6 Hz, 1H), 7.15 (d, *J* = 7.2 Hz, 1H), 7.12 – 7.08 (m, 1H), 7.05 – 7.02 (m, 1H), 6.99 – 6.89 (m, 3H), 4.70 (ABq, *J*_{AB} = 14.5 Hz, 2H), 4.54 (s, 2H), 3.36 (t, *J* = 6.6 Hz, 2H), 2.64 – 2.47 (m, 2H), 2.24 (s, 3H), 2.03 (s, 3H); ¹³C NMR (100 MHz, CDCl₃) δ 164.1, 162.4 (d, *J* = 244.9 Hz), 160.9 (d, *J* = 147.4 Hz), 139.7, 138.5 (d, *J* = 8.0 Hz), 136.7 (d, *J* = 8.7 Hz), 134.9 (d, *J* = 3.0 Hz), 133.7, 132.7 (d, *J* = 3.4 Hz), 131.4 (d, *J* = 5.2 Hz), 130.9 (d, *J* = 8.3 Hz), 130.4, 128.4, 127.2 (d, *J* = 8.0 Hz), 125.3 (d, *J* = 17.4 Hz), 116.9 (d, *J* = 21.0 Hz), 115.2

(d, $J = 22.5$ Hz), 112.9 (d, $J = 21.1$ Hz), 50.0, 45.1, 32.7, 25.7, 20.2, 14.7 (d, $J = 3.4$ Hz);
LCMS (ESI): $m/z = 470.0$ [M + H]⁺.

7-(Bromomethyl)-2-(3,5-dimethoxybenzyl)-5-(4-fluoro-2-methylphenyl)-3,4-dihydroisoquinolin-1(2H)-one (52).

General procedure E was followed using **49** (0.60 g, 1.4 mmol) to obtain the title compound (0.64 g, 93% yield). ¹H NMR (400 MHz, DMSO-*d*₆) δ 8.08 (d, $J = 1.9$ Hz, 1H), 7.40 (d, $J = 1.9$ Hz, 1H), 7.21 – 7.16 (m, 2H), 7.08 (td, $J = 8.7, 4.0$ Hz, 1H), 6.45 (d, $J = 2.2$ Hz, 2H), 6.40 (t, $J = 2.2$ Hz, 1H), 4.81 (s, 2H), 4.63 (ABq, $J_{AB} = 14.9$ Hz, 2H), 3.71 (s, 3H), 3.40 (t, $J = 6.6$ Hz, 2H), 2.68 – 2.60 (m, 1H), 2.50 – 2.43 (m, 1H), 2.03 (s, 3H); ¹³C NMR (100 MHz, DMSO-*d*₆) δ 163.0, 161.5 (d, $J = 242.4$ Hz), 160.6, 139.9, 138.9, 138.3 (d, $J = 8.0$ Hz), 136.8, 136.5, 134.9 (d, $J = 2.7$ Hz), 133.4, 131.1 (d, $J = 8.6$ Hz), 129.9, 127.8, 116.5 (d, $J = 21.0$ Hz), 112.5 (d, $J = 20.9$ Hz), 105.6, 98.7, 55.1, 49.8, 44.8, 33.7, 25.1, 19.6; LCMS (ESI): $m/z = 497.8$ [M + H]⁺.

Protein Expression and Purification.

Human WDR5 (aa: 22–334) was cloned into a modified pET27 vector (pBG104) with a 6xHis-SUMO tag present at the N terminus. The plasmid was then transformed into E. coli BL21-Gold (DE3) cells. One hundred milliliters of LB starter was used to inoculate a 10l fermentation culture (BioFlo 415, New Brunswick Scientific), grown at 37 °C. Fermentation growth media contained KH₂PO₄ (4 g/L), K₂HPO₄ (6 g/L), Na₂SO₄ (2 g/L), K₂SO₄ (1 g/L), NaCl (0.5 g/L), Yeast Extract (5 g/L), glycerol (2 ml/L), Antifoam (0.2 ml/L), 5% LB medium, glucose (25 g/L), MgCl₂ (2 mM), CaCl₂ (0.1 mM), NH₄Cl (2.5 g/L), and Kanamycin (50 μ g/ml). When the cell density reached OD₆₀₀ = 2.0, the temperature was lowered to 25 °C, and WDR5 expression induced by treatment with 1 mM isopropyl- β -D-thioga-lactoside (IPTG) overnight. Cell pellets were collected, dissolved in lysis buffer containing 1XPBS plus 300 mM NaCl, 20 mM imidazole, 5 mM BME, and 10% glycerol, and lysed by homogenization (APV-2000, APV). The lysate was cleared by centrifugation, filtered, and then applied to the Ni-column (140 mL, ProBond, Invitrogen). Bound protein was eluted using an imidazole gradient (0–500 mM). The His-SUMO-tag was cleaved by SUMO protease during dialysis and subsequently eliminated through a second Ni-column. WDR5 protein was then purified by size-exclusion chromatography (HiLoad 26/60, Superdex 75, GE Healthcare) using crystallization buffer consisting of 20 mM HEPES, pH 7.0, 250 mM NaCl, and 5 mM DTT. The purity of protein was checked using SDS-PAGE. Purified WDR5 was then concentrated to 10 mg/mL, and was stored at –80 °C.

Protein Crystallization, Data Collection, and Structure Refinement.

WDR5 apo- and co-crystals were obtained at 18 °C using the sitting drop vapor diffusion method. The crystallization condition was 0.1 M Bis-Tris or HEPES or HCl-Tris pH 6.0–8.0, 0.2 M ammonium acetate, 20% to 30% PEG3350. A soaking method was applied for some of the compounds using WDR5 apo-crystals. Crystals were flash frozen directly in liquid nitrogen. Diffraction data were collected on the Life Sciences Collaborative Access Team (LS-CAT) 21-ID-D and G beamlines at the Advanced Photon Source (APS) at Argonne National Laboratory. Diffraction data were indexed, integrated, and scaled using

HKL2000.⁴³ Molecular replacement was applied using Phaser as implemented in CCP4⁴⁴ using a published structure (PDB code 3EG6). Refinement of the structural models was performed using PHENIX⁴⁵ along with rounds of manual model building in COOT⁴⁶. All structure images were prepared with PyMOL. A summary of the final refinement statistics for structures including compounds **13** and **16** can be found in Table S1.

TR-FRET Competition Assay.

The 10-mer-Thr-FAM (ARTEVHLRKS-(Ahx-Ahx)(Lys-(5-FAM)))³⁶ peptide was purchased from GeneScript and used without additional purification. TR-FRET emissions were recorded on a BioTek Cytation 3 instrument.

For the 10-mer-Thr-FAM peptide TR-FRET assay, LanthaScreen Elite Tb-anti His antibody (Tb-Ab) was purchased from Thermo-Fisher and used at 1 nM. The 10-mer-Thr-FAM peptide was used at 150 nM, while WDR5-His-SUMO tag protein was used at 2 nM. The working assay buffer composition was modified to pH 7.2 (1X Phosphate Buffered Saline, 300 mM NaCl, 0.5 mM TCEP, 0.1% CHAPS). Stock compounds were dispensed to a white, flat-bottom OptiPlate plate (PerkinElmer) using an Echo Liquid Handler. An 11-point, Semi-log dilution scheme with a top concentration of 1 μ M (0.010 nM low concentration) was used with a final volume of 20 μ l. Both the top concentration and the dilution scheme was adjusted to fit the anticipated potency of the compounds. Using the above probe concentration and assay conditions, the calculated lower K_i limit was $\sim 0.020 \pm 0.010$ nM. Positive control wells (0% displacement) consisted of His-SUMO-WDR5 and 10-mer-Thr-FAM probe/Tb antibody mix occupying column 24, while negative control wells (100% displacement) consisting of the 10-mer-Thr-FAM probe/terbium antibody mix alone occupy column 1. The assay performed with an average Z' value of 0.7 and was found to be tolerant to up to 5% DMSO, but routinely screened at 1% DMSO.

For IC_{50} determinations, plates were covered, shielded from light, and incubated for 1h at room temperature with rocking. For the TR-FRET assay, measurement plates were excited at a wavelength of 340 nm, and emission wavelengths of 495 and 520 nm were used. The ratio of the 520/495 wavelengths were used to assess the degree of the FRET signal and resulting peptide displacement. TR-FRET plate positive control wells include column 24 containing 10-mer-Thr-FAM peptide, His-SUMO-WDR5, and Tb-anti-His antibody to measure maximum signal from the FRET response. The 520/495 emission ratio (TR-FRET) was used to calculate an IC_{50} (inhibitor concentration at which 50% of the bound peptide is displaced) by fitting the inhibition data using XLFit software (Guilford, UK) to single-site binding model. This was converted into a binding inhibition/displacement constant (K_i) using the formula:⁴⁷

$$Compound \ K_i = \frac{[I]_{50}}{\frac{[L]_{50}}{K_d^{pep}} + \frac{[P]_0}{K_d^{pep}} + 1}$$

where $[I]_{50}$ is the concentration of the free inhibitor at 50% inhibition, $[L]_{50}$ is the concentration of the free labeled ligand at 50% inhibition, $[P]_0$ is the concentration of the

free protein at 0% inhibition, and K_d^{pep} represents the dissociation constant of the 10-mer-Thr-FAM probe.

MLL1 Histone Methyltransferase Assay.

HMT inhibition activity assays (assay catalog #HMT-15-105, MLL1 complex no extra WRAD2) were performed at Reaction Biology Corporation in a HotSpot radioisotope based filter-binding format. The assay was performed using purified recombinant human MLL1 complex (total MW = 212 kDa): MLL1 (aa 3745-3969, GenBank Accession No. [NM_005933](#)), WDR5 (aa 22-334, GenBank Accession No. [NM_017588](#)), RbBP5 (aa 1-538, GenBank Accession No. [NM_005057](#)), Ash2L (aa 2-534, GenBank Accession No. [NM_001105214](#)), DPY-30 (aa 1-99, GenBank Accession No. [NM_0325742](#)), all with N-terminal His tag were expressed in E. coli, and mixed molar ratio of 1:1:1:1:2, respectively, in a reaction buffer (50 mM Tris-HCl (pH 8.5), 5 mM MgCl₂, 50 mM NaCl, 0.01% Brij35, 1 mM DTT, 1% DMSO). Purified oligonucleosomes were obtained from HeLa cells (primarily oligomers of 3-6 units, 600-1200 bp DNA), and S-adenosyl-L-[methyl-³H]methionine (SAM) was used as the methylation cofactor.⁴⁸ S-Adenosylhomocysteine (SAH) was used as a positive control. Reaction conditions consisted of 7-10 nM of MLL1 complex, 0.05 mg/mL HeLa oligonucleosomes, and 1 μM of SAM substrate. Compounds were tested in duplicate using a 10-point CRC 3-fold serial dilution from a 3 μM top concentration. See the SI and www.reactionbiology.com for further details.

Cellular Proliferation Assays.

Cell proliferation was assayed using the Promega CellTiter-Glo Luminescent Kit. White, opaque, flat-bottomed 384-well plates were used. Two hundred cells were seeded per well for all cell lines. Cells were treated with 0.3% DMSO vehicle only or 22 two-fold dilutions of WDR5 inhibitors with a top concentration of 30 μM. Final DMSO concentration was 0.3% in all compound treatment experiments and at least two biological replicates were performed. The total volume of cells with inhibitor was 32 μL per well. Thirty-two μL of sterile media was added to all of the empty wells around the edge of the plate to prevent evaporation. Plates were incubated at 37 °C, 5% CO₂ for 5 days. At the end of incubation, the plates were allowed to reach room temperature before adding 16 μL of CellTiter-Glo reagent per well. Plates were incubated at room temperature, covered from light, for 15 min before the luminescence was measured using the CellTiter-Glo protocol on a Cytation3 plate reader (BioTek, Winooski, VT). The raw luminescence values were normalized to the DMSO vehicle only wells and PRISM software or XLfit (IDBS, Guildford, United Kingdom) was used to generate GI₅₀ values. Error bars on proliferation curves represent standard errors of the mean.

WDR5 Immunoprecipitation.

40×10^6 MV4:11 cells were resuspended in 8 mL of media and treated for 4 h with DMSO or 1 μM compound **16**. Cell lysates were prepared in IP buffer [50 mM Tris-HCl pH 8.0, 150 mM NaCl, 5 mM EDTA, 1% Triton X-100] plus Complete Protease Inhibitor Cocktail (Roche), briefly sonicated, and cleared by centrifugation. Immune complexes were precipitated overnight at 4 °C with the normal rabbit IgG or anti-WDR5 antibody (Bethyl),

captured for 2 h at 4 °C with Protein-A Agarose (Sigma), washed four times in IP buffer, and resolved by SDS-PAGE. Antibodies used for immunoblotting were MLL1 and WDR5 from Cell Signaling Technologies, and RBBP5 from Bethyl.

Chromatin Immunoprecipitation.

Chromatin immunoprecipitation (ChIP) assays were performed as previously described.¹⁴ Cells were treated with 0.1% DMSO or 600 nM compound **16** for 4 h at 37 °C, then washed in PBS and cross-linked with 1% formaldehyde at room temperature for 10 min. The reaction was quenched with 125 mM glycine for 10 min at room temperature, then cells were washed with ice cold PBS. Cells were lysed in Formaldehyde Lysis Buffer (50 mM HEPES pH 7.5, 140 mM NaCl, 1 mM EDTA, 1% Triton, 1% SDS, and Complete Protease Inhibitor cocktail) using 250 μL of buffer per 1×10^7 cells, on ice, for 10 min. Chromatin was sheared by 25-min sonication (BioRuptor) to yield a mean chromatin size of ~ 250 bp, and debris cleared by centrifugation. Sheared chromatin was diluted 10-fold in Formaldehyde Lysis Buffer without SDS before immunoprecipitation overnight at 4 °C using the appropriate antibody and Protein A agarose. Chromatin from 6 million cells was used per reaction. Immune complexes were washed sequentially with Low Salt Wash buffer (20 mM Tris pH 8.0, 150 mM NaCl, 2 mM EDTA, 1% Triton), High Salt Wash Buffer (20 mM Tris pH 8.0, 500 mM NaCl, 2 mM EDTA, 1% Triton), LiCl Wash buffer (25 mM LiCl, 1 mM EDTA, 1% Triton) and twice with TE (pH 8.0). Protein–DNA complexes were de-crosslinked overnight at 65 °C in Elution Buffer (TE, 0.1% SDS, 40 μg Proteinase K). Proteinase K was heat inactivated for 20 min at 95 °C then 150 μL of TE was added. 1 μL of DNA was used in a 15 μL PCR reaction using KAPA SYBR FAST qPCR Master Mix 2X Universal and quantified on an Eppendorf Realplex2 Mastercycler in triplicate. ChIP signals were calculated as percent input. ChIP experiments were completed in biological triplicate with error bars representing the standard error of the mean.

RT-qPCR Quantification of mRNA Expression.

MV4:11 cells were treated for three days with 0.1% DMSO or 300 nM compound **16**. Cells were then lysed in 500 μL Trizol, and total RNA was extracted using the Zymo Research Direct-zol RNA MiniPrep kit with on-column DNase digestion. After extraction, 1 μg of RNA was reverse transcribed using MuLV reverse transcriptase (Life Tech N8080018) in 20 μL reaction, then diluted three-fold with nuclease-free water. 1 μL of cDNA was used in a 15 μL qPCR reaction using KAPA SYBR FAST qPCR Master Mix 2X Universal and quantified on an Eppendorf Realplex2 Mastercycler in triplicate. Relative mRNA expression of genes of interest was quantified using the CT method, normalizing to the signal from GAPDH. mRNA expression studies were completed in triplicate with error bars representing the standard error of the mean.

Caspase Assay.

MV4–11 cells were incubated with compounds in 384 well plates at in a 32 μL volume containing 1600 cells. A 16 μL volume of Caspase-Glo® 3/7 reagent (Promega Biosciences, Madison WI) was added and luminescence was measured using a Cytation 3 plate reader.

Cell Cycle Analysis.

4 million cells were treated for three days with the indicated amount of compound. Cell pellets were permeabilized in 70% Ethanol for 1 hour at 4 °C, washed twice with PBS, incubated for 5 minutes in 50 µL PBS containing 5 µg RNase A (Qiagen), then stained by adding 450 µL PBS and propidium iodide (Sigma) to 1 µg/mL. Cell cycle analysis was then carried out using an LSRII Flow Cytometer and data was analyzed with FACSDiva software (BD Biosciences).

Western Blot.

Compound treated cells were lysed in RIPA containing protease and phosphatase inhibitor cocktail. Changes in protein levels were measured by western blot using monoclonal antibodies against p53 (DO-1, Santa Cruz Biotechnology), p21 (12D1, Cell Signaling Technology, Danvers, MA), and GAPDH (14C10, Cell Signaling Technology).

Colorectal CTOSs Assays.

CTOSs were prepared and cultured as described previously.^{36, 37} CTOSs were cultured with StemPro hESC medium (Invitrogen) at 37 °C with 5% CO₂. For the sensitivity assays for compound **1** and **16**, CTOSs were dissociated into single cells using TrypLE express (Invitrogen) and filtered through a 35 µm cell strainer (BD Falcon). Cell suspension in Matrigel (Corning) at 200–400 cells/µl were prepared, and 5µl of Matrigel drop containing cancer cells were put in wells of 96-well plates. After the gels solidified, StemPro medium with indicated concentration of drugs were applied. Following 7 to 9 days of culture, viability of the cultured cells was evaluated by Celltiter-Glo (Promega).

Supplementary Material

Refer to Web version on PubMed Central for supplementary material.

ACKNOWLEDGMENT

We thank the Vanderbilt High-Throughput Screening Core facility for compound management and Vanderbilt University Biomolecular NMR Facility for use of Bruker NMR spectrometers. This facility receives support from an NIH SIG Grant (1S-10RR025677-01) and Vanderbilt University matching funds. The authors also thank contributing and supporting members of Leidos Biomedical Research at Frederick National Labs for Cancer Research, Reaction Biology Corp. and the NCI Chemical Biology Consortium. Use of the Advanced Photon Source, an Office of Science User Facility operated for the US Department of Energy Office of Science by the Argonne National Laboratory, was supported by US Department of Energy [Contract No. DE-AC02-06CH11357]. Use of the Life Sciences Collaborative Access Team Sector 21 was supported by the Michigan Economic Development Corporation and Michigan Technology Tri- Corridor Grant [grant number 085P1000817]. This work was also funded by NCI/NIH CA211305 to L.R.T.

Funding Sources

This work was generously supported in part with Federal funds from the National Cancer Institute, National Institutes of Health, under Chemical Biology Consortium Contract No. HHSN261200800001E (to S.W.F), grant CA200709 from the National Institutes of Health (to W.P.T), The Vanderbilt Ingram Cancer Center Support grant (NIH: CA68485), GI Special Programs in Research Excellence P50 CA236733 and startup funds to S.W.F. provided by Vanderbilt University. This work was also supported by grants from the Robert J. Kleberg, Jr., and Helen C. Kleberg Foundation (to WPT and SWF), The TJ Martell Foundation (to W.P.T. and S.W.F.), St. Baldrick's Foundation (W.P.T.), Alex's Lemonade Stand Foundation (W.P.T.), Edward P. Evans Foundation (W.P.T.), the NCI/NIH (CA211305; L.R.T.), and the IBSTO Training Program (T32 CA119925; E.R.A./W.P.T.). The content of this publication does not necessarily reflect the views or policies of the Department of Health and Human Services,

nor does mention of trade names, commercial products, or organizations imply endorsement by the U.S. Government.

ABBREVIATIONS USED

ALL	acute lymphoid leukemia
AML	acute myeloid leukemia
C/EBPα	CCAAT-enhancer-binding protein α
ChIP	chromatin immunoprecipitation
CTOSs	cancer tissue-originated spheroids
GI₅₀	half-maximal growth inhibition
HMT	histone methyltransferases
K_i	binding inhibition constant
MLL	Mixed-Lineage Leukemia
TR-FRET	time-resolved fluorescence energy transfer
WDR5	WD repeat domain 5 protein
WIN	WDR5 interaction motif

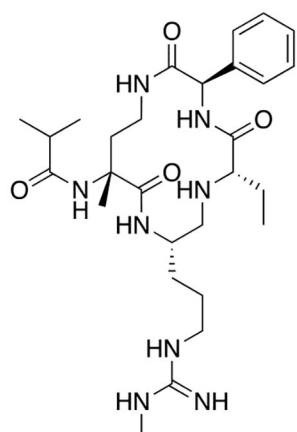
REFERENCES

- (1). Smith TF; Gaitatzes C; Saxena K; Neer EJ The WD Repeat: A Common Architecture for Diverse Functions. *Trends Biochem. Sci* 1999, 24 (5), 181–185. [PubMed: 10322433]
- (2). Stirnimann CU; Petsalaki E; Russell RB; Müller CW WD40 Proteins Propel Cellular Networks. *Trends Biochem. Sci* 2010, 35 (10), 565–574. [PubMed: 20451393]
- (3). Xu C; Min J Structure and Function of WD40 Domain Proteins. *Protein Cell* 2011, 2 (3), 202–214. [PubMed: 21468892]
- (4). Guarnaccia A; Tansey W; Guarnaccia AD; Tansey WP Moonlighting with WDR5: A Cellular Multitasker. *J. Clin. Med* 2018, 7 (2), 21.
- (5). Dai X; Guo W; Zhan C; Liu X; Bai Z; Yang Y WDR5 Expression Is Prognostic of Breast Cancer Outcome. *PLoS One* 2015, 10 (9), e0124964. [PubMed: 26355959]
- (6). Zhu J; Sammons MA; Donahue G; Dou Z; Vedadi M; Getlik M; Barsyte-Lovejoy D; Al-awar R; Katona BW; Shilatifard A; Huang J; Hua X; Arrowsmith CH; Berger SL Gain-of-Function P53 Mutants Co-Opt Chromatin Pathways to Drive Cancer Growth. *Nature* 2015, 525 (7568), 206–211. [PubMed: 26331536]
- (7). Wang F; Jeon KO; Salovich JM; Macdonald JD; Alvarado J; Gogliotti RD; Phan J; Olejniczak ET; Sun Q; Wang S; Camper D; Yuh JP; Shaw JG; Sai J; Rossanese OW; Tansey WP; Stauffer SR; Fesik SW Discovery of Potent 2-Aryl-6,7-Dihydro-5 H-Pyrrolo[1,2- a]Imidazoles as WDR5-WIN-Site Inhibitors Using Fragment-Based Methods and Structure-Based Design. *J. Med. Chem* 2018, 61 (13), 5623–5642. [PubMed: 29889518]
- (8). Aho ER; Wang J; Gogliotti RD; Howard GC; Phan J; Acharya P; Macdonald JD; Cheng K; Lorey SL; Lu B; Wenzel S; Foshage AM; Alvarado J; Wang F; Shaw JG; Zhao B; Weissmiller AM; Thomas LR; Vakoc CR; Hall MD; Hiebert SW; Liu Q; Stauffer SR; Fesik SW; Tansey WP Displacement of WDR5 from Chromatin by a WIN Site Inhibitor with Picomolar Affinity. *Cell Rep.* 2019, 26 (11), 2916–2928. [PubMed: 30865883]

- (9). Patel A; Dharmarajan V; Cosgrove MS Structure of WDR5 Bound to Mixed Lineage Leukemia Protein-1 Peptide. *J. Biol. Chem* 2008, 283 (47), 32158–32161. [PubMed: 18829459]
- (10). Patel A; Vought VE; Dharmarajan V; Cosgrove MS A Conserved Arginine-Containing Motif Crucial for the Assembly and Enzymatic Activity of the Mixed Lineage Leukemia Protein-1 Core Complex. *J. Biol. Chem* 2008, 283 (47), 32162–32175. [PubMed: 18829457]
- (11). Hess JL MLL: A Histone Methyltransferase Disrupted in Leukemia. *Trends Mol. Med* 2004, 10 (10), 500–507. [PubMed: 15464450]
- (12). Dharmarajan V; Lee J-H; Patel A; Skalnik DG; Cosgrove MS Structural Basis for WDR5 Interaction (Win) Motif Recognition in Human SET1 Family Histone Methyltransferases. *J. Biol. Chem* 2012, 287 (33), 27275–27289. [PubMed: 22665483]
- (13). Alicea-Velázquez NL; Shinsky SA; Loh DM; Lee JH; Skalnik DG; Cosgrove MS Targeted Disruption of the Interaction between WD-40 Repeat Protein 5 (WDR5) and Mixed Lineage Leukemia (MLL)/SET1 Family Proteins Specifically Inhibits MLL1 and SET1A Methyltransferase Complexes. *J. Biol. Chem* 2016, 291 (43), 22357–22372. [PubMed: 27563068]
- (14). Thomas LR; Wang Q; Grieb BC; Phan J; Foshage AM; Sun Q; Olejniczak ET; Clark T; Dey S; Lorey S; Alicie B; Howard GC; Cawthon B; Ess KC; Eischen CM; Zhao Z; Fesik SW; Tansey WP Interaction with WDR5 Promotes Target Gene Recognition and Tumorigenesis by MYC. *Mol. Cell* 2015, 58 (3), 440–452. [PubMed: 25818646]
- (15). Chen X; Xie W; Gu P; Cai Q; Wang B; Xie Y; Dong W; He W; Zhong G; Lin T; Huang J Upregulated WDR5 Promotes Proliferation, Self-Renewal and Chemoresistance in Bladder Cancer via Mediating H3K4 Trimethylation. *Sci. Rep* 2015, 5 (1), 8293. [PubMed: 25656485]
- (16). Carugo A; Genovese G; Seth S; Nezi L; Rose JL; Bossi D; Cicalese A; Shah PK; Viale A; Pettazzoni PF; Akdemir KC; Bristow CA; Robinson FS; Tepper J; Sanchez N; Gupta S; Estecio MR; Giuliani V; Dellino GI; Riva L; Yao W; Di Francesco ME; Green T; D'Alesio C; Corti D; Kang Y; Jones P; Wang H; Fleming JB; Maitra A; Pelicci PG; Chin L; DePinho RA; Lanfrancone L; Heffernan TP; Draetta GF In Vivo Functional Platform Targeting Patient-Derived Xenografts Identifies WDR5-Myc Association as a Critical Determinant of Pancreatic Cancer. *Cell Rep.* 2016, 16 (1), 133–147. [PubMed: 27320920]
- (17). Tan X; Chen S; Wu J; Lin J; Pan C; Ying X; Pan Z; Qiu L; Liu R; Geng R; Huang W PI3K/AKT-Mediated Upregulation of WDR5 Promotes Colorectal Cancer Metastasis by Directly Targeting ZNF407. *Cell Death Dis.* 2017, 8 (3), e2686–e2686. [PubMed: 28300833]
- (18). Sun W; Guo F; Liu M Up-Regulated WDR5 Promotes Gastric Cancer Formation by Induced Cyclin D1 Expression. *J. Cell. Biochem* 2018, 119 (4), 3304–3316. [PubMed: 29125890]
- (19). Malek R; Gajula RP; Williams RD; Nghiem B; Simons BW; Nugent K; Wang H; Taparra K; Lemtiri-Chlieh G; Yoon AR; True L; An SS; DeWeese TL; Ross AE; Schaeffer EM; Pienta KJ; Hurley PJ; Morrissey C; Tran PT TWIST1-WDR5- *Hottip* Regulates *Hoxa9* Chromatin to Facilitate Prostate Cancer Metastasis. *Cancer Res.* 2017, 77 (12), 3181–3193. [PubMed: 28484075]
- (20). Tran PT; Gajula R; Williams R; Malek R; Nugent K; Walker A; Chettiar S; Wang H; Taparra K; Cades J; Herman J A Twist1-MLL-WDR5-HOTTIP Complex Regulates HOXA9 Chromatin to Facilitate Metastasis of Prostate Cancer. *Int. J. Radiat. Oncol* 2014, 90 (1), S177.
- (21). Sun Y; Bell JL; Carter D; Gherardi S; Poulos RC; Milazzo G; Wong JWH; Al-Awar R; Tee AE; Liu PY; Liu B; Atmadibrata B; Wong M; Trahair T; Zhao Q; Shohet JM; Haupt Y; Schulte JH; Brown PJ; Arrowsmith CH; Vedadi M; MacKenzie KL; Huttelmaier S; Perini G; Marshall GM; Braithwaite A; Liu T WDR5 Supports an N-Myc Transcriptional Complex That Drives a Protumorigenic Gene Expression Signature in Neuroblastoma. *Cancer Res.* 2015, 75 (23), 5143–5154. [PubMed: 26471359]
- (22). Wu Y; Diao P; Li Z; Zhang W; Wang D; Wang Y; Cheng J Overexpression of WD Repeat Domain 5 Associates with Aggressive Clinicopathological Features and Unfavorable Prognosis in Head Neck Squamous Cell Carcinoma. *J. Oral Pathol. Med* 2018, 47 (5), 502–510. [PubMed: 29569374]
- (23). Ge Z; Song EJ; Kawasaki YI; Li J; Dovat S; Song C; Ge Z; Song EJ; Kawasaki YI; Li J; Dovat S; Song C WDR5 High Expression and Its Effect on Tumorigenesis in Leukemia. *Oncotarget* 2016, 7 (25), 37740–37754. [PubMed: 27192115]

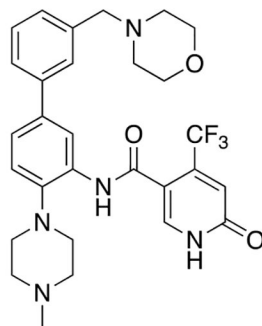
- (24). Lu K; Tao H; Si X; Chen Q The Histone H3 Lysine 4 Presenter WDR5 as an Oncogenic Protein and Novel Epigenetic Target in Cancer. *Front. Oncol* 2018, 8, 502. [PubMed: 30488017]
- (25). Meyer C; Hofmann J; Burmeister T; Gröger D; Park TS; Emerenciano M; Pombo de Oliveira M; Renneville A; Villarese P; Macintyre E; Cavé H; Clappier E; Mass-Malo K; Zuna J; Trka J; De Braekeleer E; De Braekeleer M; Oh SH; Tsaur G; Fechina L; van der Velden VHJ; van Dongen JJM; Delabesse E; Binato R; Silva MLM; Kustanovich A; Aleinikova O; Harris MH; Lund-Aho T; Juvonen V; Heidenreich O; Vormoor J; Choi WWL; Jarosova M; Kolenova A; Bueno C; Menendez P; Wehner S; Eckert C; Talmant P; Tondeur S; Lippert E; Launay E; Henry C; Ballerini P; Lapillone H; Callanan MB; Cayuela JM; Herbaux C; Cazzaniga G; Kakadiya PM; Bohlander S; Ahlmann M; Choi JR; Gameiro P; Lee DS; Krauter J; Cornillet-Lefebvre P; Te Kronnie G; Schäfer BW; Kubetzko S; Alonso CN; zur Stadt U; Sutton R; Venn NC; Izraeli S; Trakhtenbrot L; Madsen HO; Archer P; Hancock J; Cerveira N; Teixeira MR; Lo Nigro L; Mörcke A; Stanulla M; Schrappe M; Sedék L; Szczepa ski T; Zwaan CM; Coenen EA; van den Heuvel-Eibrink MM; Strehl S; Dworzak M; Panzer-Grümayer R; Dingermann T; Klingebiel T; Marschalek R The MLL Recombinome of Acute Leukemias in 2013. *Leukemia* 2013, 27 (11), 2165–2176. [PubMed: 23628958]
- (26). Muntean AG; Hess JL The Pathogenesis of Mixed-Lineage Leukemia. *Annu. Rev. Pathol. Mech. Dis* 2012, 7 (1), 283–301.
- (27). Winters AC; Bernt KM MLL-Rearranged Leukemias—An Update on Science and Clinical Approaches. *Front. Pediatr* 2017, 5, 4. [PubMed: 28232907]
- (28). Krivtsov AV; Armstrong SA MLL Translocations, Histone Modifications and Leukaemia Stem-Cell Development. *Nat. Rev. Cancer* 2007, 7 (11), 823–833. [PubMed: 17957188]
- (29). Cao F; Townsend EC; Karatas H; Xu J; Li L; Lee S; Liu L; Chen Y; Ouillette P; Zhu J; Hess JL; Atadja P; Lei M; Qin ZS; Malek S; Wang S; Dou Y Targeting MLL1 H3K4 Methyltransferase Activity in Mixed-Lineage Leukemia. *Mol. Cell* 2014, 53 (2), 247–261. [PubMed: 24389101]
- (30). Chen Y; Anastassiadis K; Kranz A; Stewart AF; Arndt K; Waskow C; Yokoyama A; Jones K; Neff T; Lee Y; Ernst P MLL2, Not MLL1, Plays a Major Role in Sustaining MLL-Rearranged Acute Myeloid Leukemia. *Cancer Cell* 2017, 31 (6), 755–770. [PubMed: 28609655]
- (31). Aho ER; Weissmiller AM; Fesik SW; Tansey WP Targeting WDR5: A WINning Anti-Cancer Strategy? *Epigenetics insights* 2019, 12, 1–5.
- (32). Karatas H; Li Y; Liu L; Ji J; Lee S; Chen Y; Yang J; Huang L; Bernard D; Xu J; Townsend EC; Cao F; Ran X; Li X; Wen B; Sun D; Stuckey JA; Lei M; Dou Y; Wang S Discovery of a Highly Potent, Cell-Permeable Macrocyclic Peptidomimetic (MM-589) Targeting the WD Repeat Domain 5 Protein (WDR5)–Mixed Lineage Leukemia (MLL) Protein–Protein Interaction. *J. Med. Chem* 2017, 60 (12), 4818–4839. [PubMed: 28603984]
- (33). Grebien F; Vedadi M; Getlik M; Giamb Bruno R; Grover A; Avellino R; Skucha A; Vittori S; Kuznetsova E; Smil D; Barsyte-Lovejoy D; Li F; Poda G; Schapira M; Wu H; Dong A; Senisterra G; Stukalov A; Huber KVM; Schönegger A; Marcellus R; Bilban M; Bock C; Brown PJ; Zuber J; Bennett KL; Al-awar R; Delwel R; Nerlov C; Arrowsmith CH; Superti-Furga G Pharmacological Targeting of the Wdr5-MLL Interaction in C/EBP α N-Terminal Leukemia. *Nat. Chem. Biol* 2015, 11 (8), 571–578. [PubMed: 26167872]
- (34). Getlik M; Smil D; Zepeda-Velázquez C; Bolshan Y; Poda G; Wu H; Dong A; Kuznetsova E; Marcellus R; Senisterra G; Dombrowski L; Hajian T; Kiyota T; Schapira M; Arrowsmith CH; Brown PJ; Vedadi M; Al-awar R Structure-Based Optimization of a Small Molecule Antagonist of the Interaction Between WD Repeat-Containing Protein 5 (WDR5) and Mixed-Lineage Leukemia 1 (MLL1). *J. Med. Chem* 2016, 59 (6), 2478–2496. [PubMed: 26958703]
- (35). Wang F; Jeon KO; Salovich JM; Macdonald JD; Alvarado J; Gogliotti RD; Phan J; Olejniczak ET; Sun Q; Wang S; Camper D; Yuh JP; Shaw JG; Sai J; Rossanese OW; Tansey WP; Stauffer SR; Fesik SW Discovery of Potent 2-Aryl-6,7-Dihydro-5 H -Pyrrolo[1,2- a]Imidazoles as WDR5-WIN-Site Inhibitors Using Fragment-Based Methods and Structure-Based Design. *J. Med. Chem* 2018, 61 (13), 5623–5642. [PubMed: 29889518]
- (36). Karatas H; Townsend EC; Bernard D; Dou Y; Wang S Analysis of the Binding of Mixed Lineage Leukemia 1 (MLL1) and Histone 3 Peptides to WD Repeat Domain 5 (WDR5) for the Design of Inhibitors of the MLL1–WDR5 Interaction. *J. Med. Chem* 2010, 53 (14), 5179–5185. [PubMed: 20575550]

- (37). Kondo J; Endo H; Okuyama H; Ishikawa O; Iishi H; Tsujii M; Ohue M; Inoue M Retaining Cell-Cell Contact Enables Preparation and Culture of Spheroids Composed of Pure Primary Cancer Cells from Colorectal Cancer. *Proc. Natl. Acad. Sci. U. S. A* 2011, 108 (15), 6235–6240. [PubMed: 21444794]
- (38). Kondo J; Ekawa T; Endo H; Yamazaki K; Tanaka N; Kukita Y; Okuyama H; Okami J; Imamura F; Ohue M; Kato K; Nomura T; Kohara A; Mori S; Dan S; Inoue M High-Throughput Screening in Colorectal Cancer Tissue-Originated Spheroids. *Cancer Sci.* 2019, 110 (1), 345–355. [PubMed: 30343529]
- (39). Yang H; Medeiros PF; Raha K; Elkins P; Lind KE; Lehr R; Adams ND; Burgess JL; Schmidt SJ; Knight SD; Auger KR; Schaber MD; Franklin GJ; Ding Y; DeLorey JL; Centrella PA; Mataruse S; Skinner SR; Clark MA; Cuzzo JW; Evindar G Discovery of a Potent Class of PI3K α Inhibitors with Unique Binding Mode via Encoded Library Technology (ELT). *ACS Med. Chem. Lett* 2015, 6 (5), 531–536. [PubMed: 26005528]
- (40). Bia H; Bailey S; Bhumralkar DR; Bi FC; Guo F; He M; Humphries PS; Ling AL; Lou J; Nukul S; Zhou R Fused Phenyl Amido Heterocyclic Compounds. US Patent 7,842,713, 11 30, 2010.
- (41). Vita M; Henriksson M The Myc Oncoprotein as a Therapeutic Target for Human Cancer. *Semin. Cancer Biol.* 2006, 16 (4), 318–330. [PubMed: 16934487]
- (42). van Riggelen J; Yetil A; Felsher DW MYC as a Regulator of Ribosome Biogenesis and Protein Synthesis. *Nat. Rev. Cancer* 2010, 10 (4), 301–309. [PubMed: 20332779]
- (43). Otwinowski Z; Minor W [20] Processing of X-Ray Diffraction Data Collected in Oscillation Mode. *Methods Enzymol.* 1997, 276, 307–326.
- (44). Winn MD; Ballard CC; Cowtan KD; Dodson EJ; Emsley P; Evans PR; Keegan RM; Krissinel EB; Leslie AGW; McCoy A; McNicholas SJ; Murshudov GN; Pannu NS; Potterton EA; Powell HR; Read RJ; Vagin A; Wilson KS Overview of the CCP4 Suite and Current Developments. *Acta Crystallogr. Sect. D Biol. Crystallogr* 2011, 67 (4), 235–242. [PubMed: 21460441]
- (45). Adams PD; Grosse-Kunstleve RW; Hung L-W; Ioerger TR; McCoy AJ; Moriarty NW; Read RJ; Sacchettini JC; Sauter NK; Terwilliger TC *PHENIX*: Building New Software for Automated Crystallographic Structure Determination. *Acta Crystallogr. Sect. D Biol. Crystallogr* 2002, 58 (11), 1948–1954. [PubMed: 12393927]
- (46). Emsley P; Cowtan K *Coot*: Model-Building Tools for Molecular Graphics. *Acta Crystallogr. Sect. D Biol. Crystallogr* 2004, 60 (12), 2126–2132. [PubMed: 15572765]
- (47). Nikolovska-Coleska Z; Wang R; Fang X; Pan H; Tomita Y; Li P; Roller PP; Krajewski K; Saito NG; Stuckey JA; Wang S Development and Optimization of a Binding Assay for the XIAP BIR3 Domain Using Fluorescence Polarization. *Anal. Biochem* 2004, 332 (2), 261–273. [PubMed: 15325294]
- (48). Ferry JJ; Smith RF; Denney N; Walsh CP; McCauley L; Qian J; Ma H; Horiuchi KY; Howitz KT Development and Use of Assay Conditions Suited to Screening for and Profiling of SET-Domain-Targeted Inhibitors of the MLL/SET1 Family of Lysine Methyltransferases. *Assay Drug Dev. Technol* 2015, 13 (4), 221–234. [PubMed: 26065558]



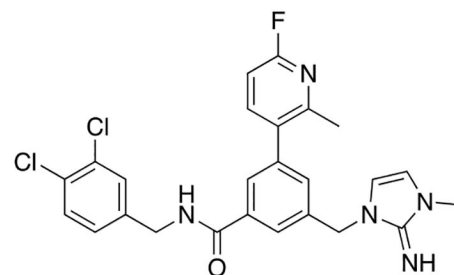
MM-589

$K_i = <1$ nM
 MLL1 HMT $IC_{50} = 13$ nM
 MV4:11 $IC_{50} = 250$ nM
 Molm13 $IC_{50} = 210$ nM



OICR-9429

$K_i = 64$ nM



1

TR-FRET $K_i = 0.044 \pm 0.008$ nM
 MLL1 HMT $IC_{50} = 20 \pm 9.6$ nM
 MV4:11 $GI_{50} = 600 \pm 150$ nM
 Molm13 $GI_{50} = 900 \pm 220$ nM
 K562 $GI_{50} = 17000 \pm 3800$ nM

Figure 1. Chemical structures and *in vitro* profiles of three previously reported WDR5-WIN-site inhibitors.

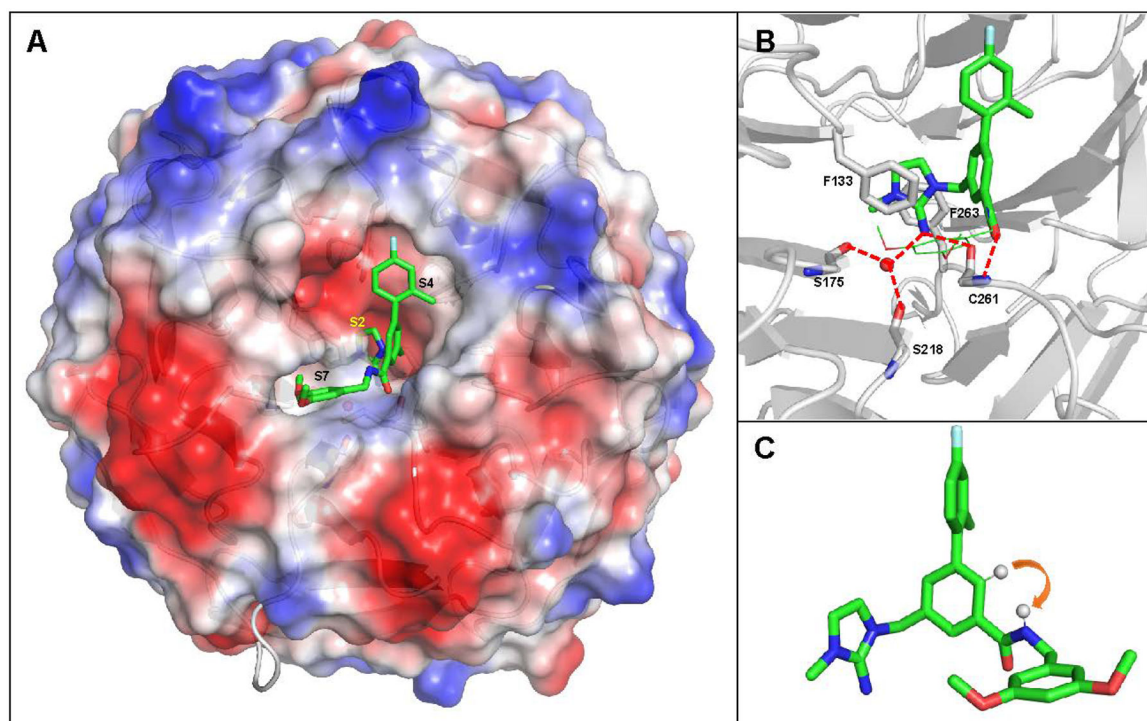


Figure 2. X-ray co-crystal structure of **13** bound to WDR5 (PDB ID: 6UFX). **(A)** Compound **13** (green-carbon capped sticks) bound to WDR5 represented as semi-transparent electrostatic potential surface with S2, S4, and S7 binding regions denoted. **(B)** Key H-bond (red dashed lines) and π - π stacking interaction residues of WDR5 that interact with **13**. **(C)** Compound **13** with hydrogen atoms highlighting the design of the bicyclic dihydroisoquinolinone core.

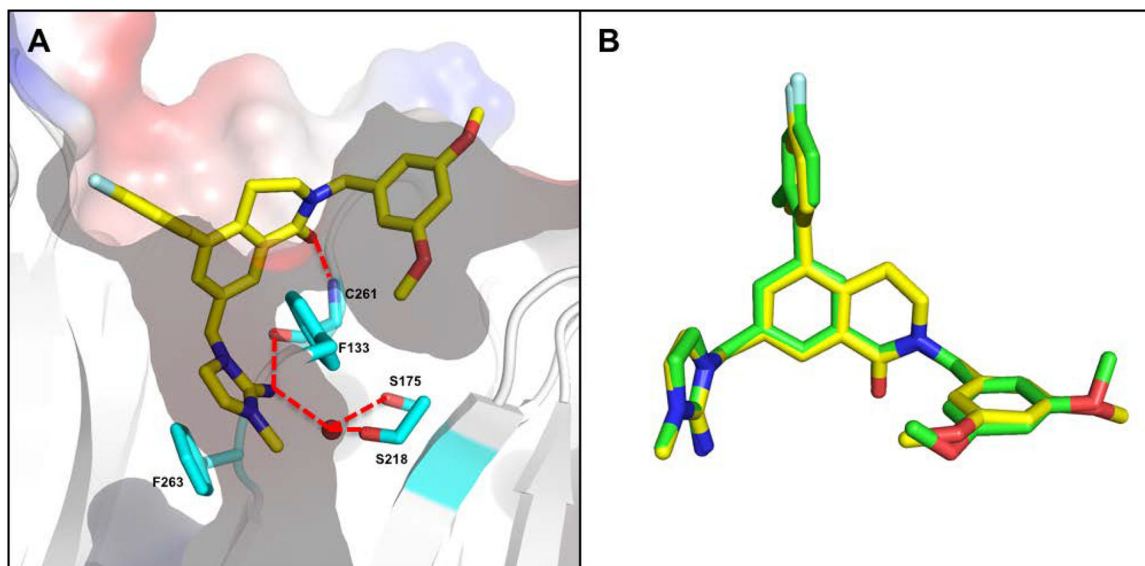


Figure 3.
X-ray co-crystal structure of **16** bound to the WDR5 WIN-site (side-view, PDB ID: 6UCS).
(A) Key H-bond (red dashed lines) and π - π stacking interaction residues of WDR5 that interact with **16**. (B) Overlay of **13** (green sticks) and **16** (yellow sticks).

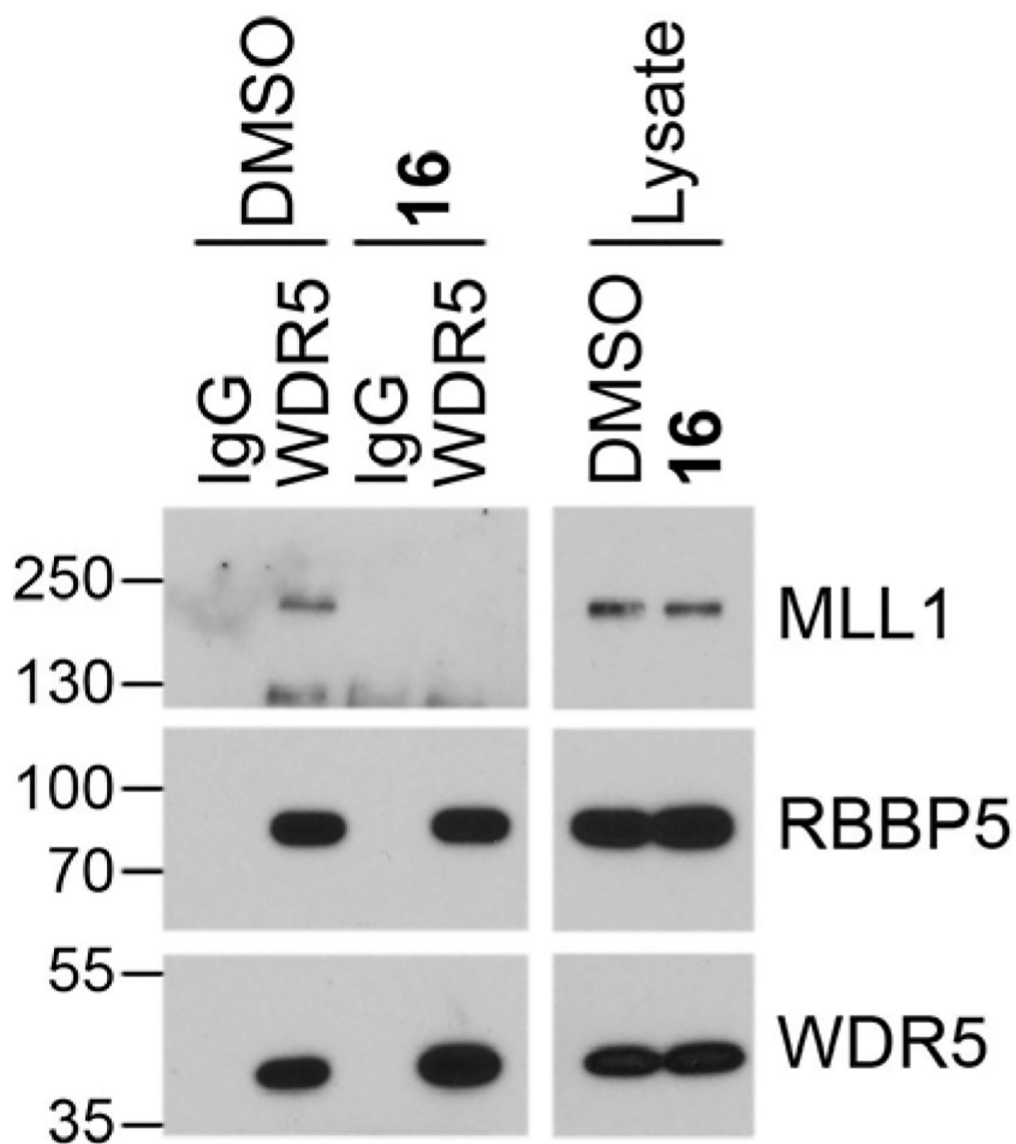


Figure 4. Compound **16** displaced MLL1 from the WRAD protein complex. Endogenous immunoprecipitation (IP) using anti-WDR5 antibody or control IgG in MV4:11 cells treated for 4 h with DMSO or 1 μ M **16**. IP'ed material and whole cell lysates were probed with MLL1, RBBP5 and WDR5 antibodies.

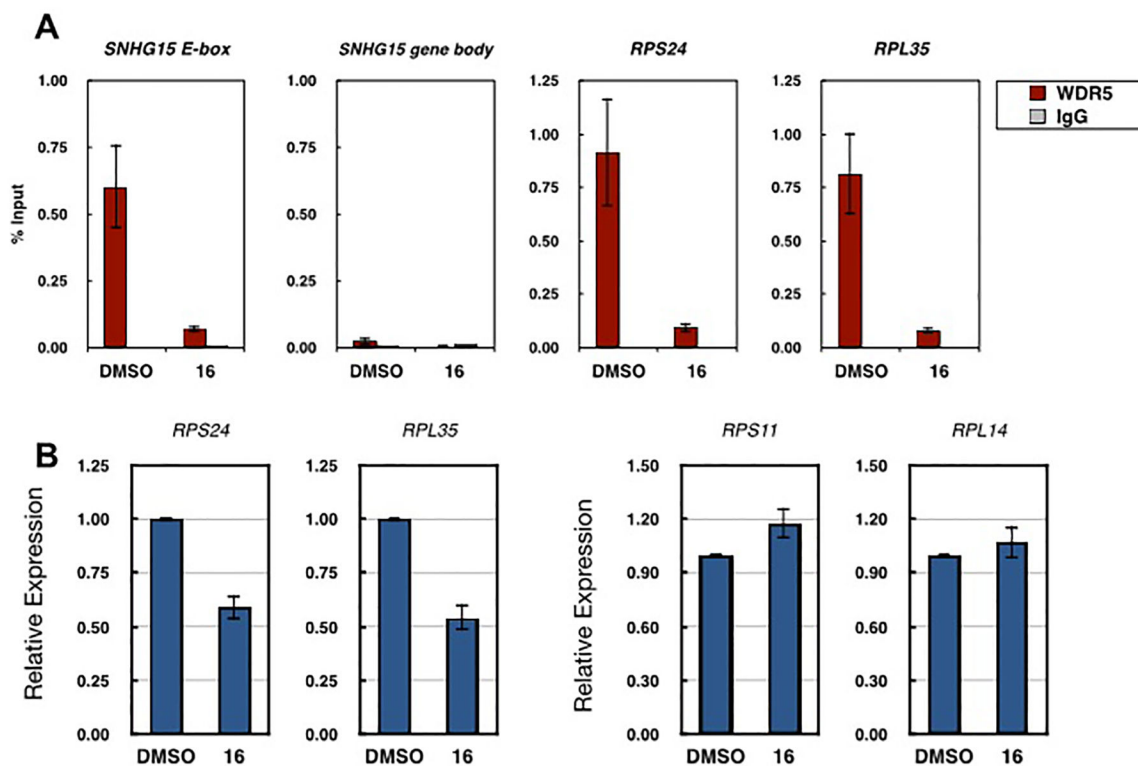


Figure 5.

Compound **16** displaced WDR5 from chromatin and repressed mRNA expression of WDR5-bound genes. **(A)** WDR5 or IgG control ChIP at three representative genes bound by WDR5 *SNHG15* (*E-box locus*), *RPS24* and *RPL35* in MV4:11 cells after 4 h treatment with 0.1% DMSO or 600 nM **16**. The *SNHG15 gene body* locus serves as a negative control for WDR5 binding, $n = 3$. **(B)** Relative mRNA expression of two-representative WDR5-bound ribosomal protein genes (*RPS24* and *RPL35*) and two representative ribosomal genes not bound by WDR5 (*RPS11* and *RPL14*) in MV4:11 cells after three-day treatment with 0.1% DMSO or 300 nM **16**, as determined by RT-qPCR. Relative expression is normalized to DMSO treatment for each gene, $n = 3$.

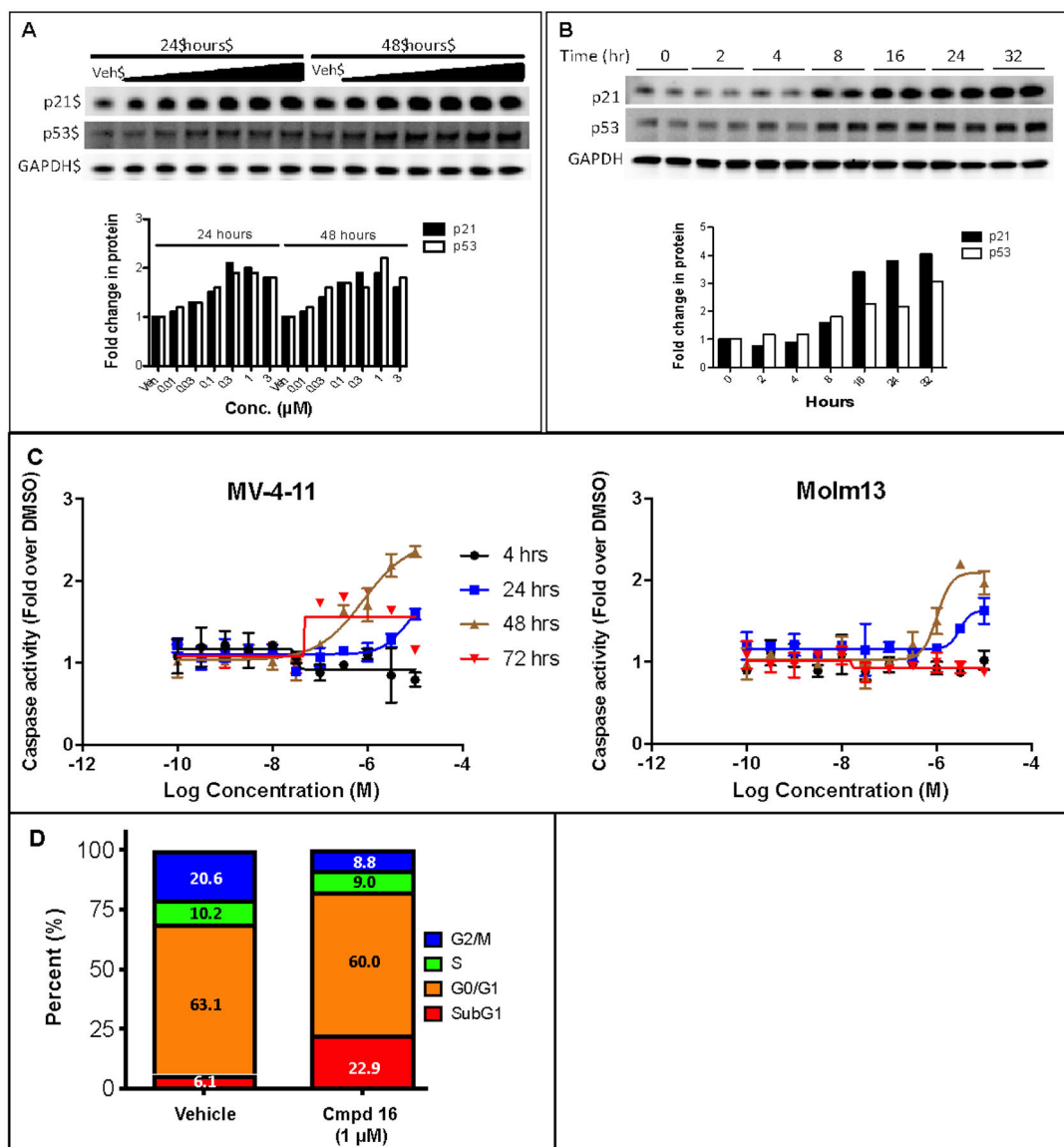


Figure 6. Compound **16** treatment induced p53 and p21 protein levels and apoptosis. **(A)** Western blot, showing the effects of DMSO or compound **16** (0.01 – 3.0 μM) on p53 and p21 protein levels in MV4:11 cells at 24h and 48h post treatment. GAPDH is a loading control. **(B)** Western blot, showing the effects of DMSO or compound **16** (0.3 μM) on p53 and p21 protein levels in MV4:11 cells in time course. GAPDH is a loading control. **(C)** Caspase 3/7 induction by compound **16** at 4, 24, 48, and 72 h time points in MV4:11 and Molm13 cells. **(D)** Cell cycle analysis of MV4:11 cells, showing 4-fold increased SubG1 cells by compound **16** treatment for 48 hours compared to DMSO control.

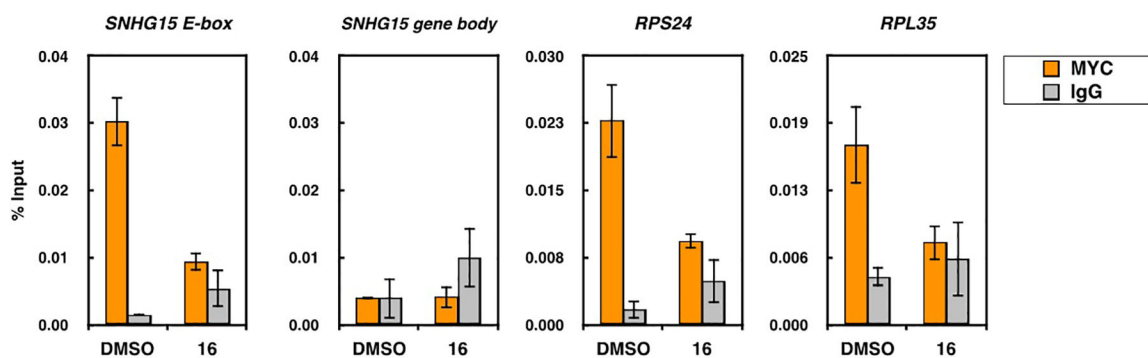


Figure 7.

Compound **16** displaces MYC from chromatin at WDR5-displaced genes. MYC or IgG control ChIP at three representative genes, *SNHG15 (E-box locus)*, *RPS24* and *RPL35*, at which **16** displaces WDR5 (as shown in Figure 5A), in MV4:11 cells. MYC or IgG control ChIPs were performed in MV4:11 cells after 4 h treatment with 0.1% DMSO or 600 nM **16**. The *SNHG15 gene body* locus serves as a negative control for MYC binding. n = 3.

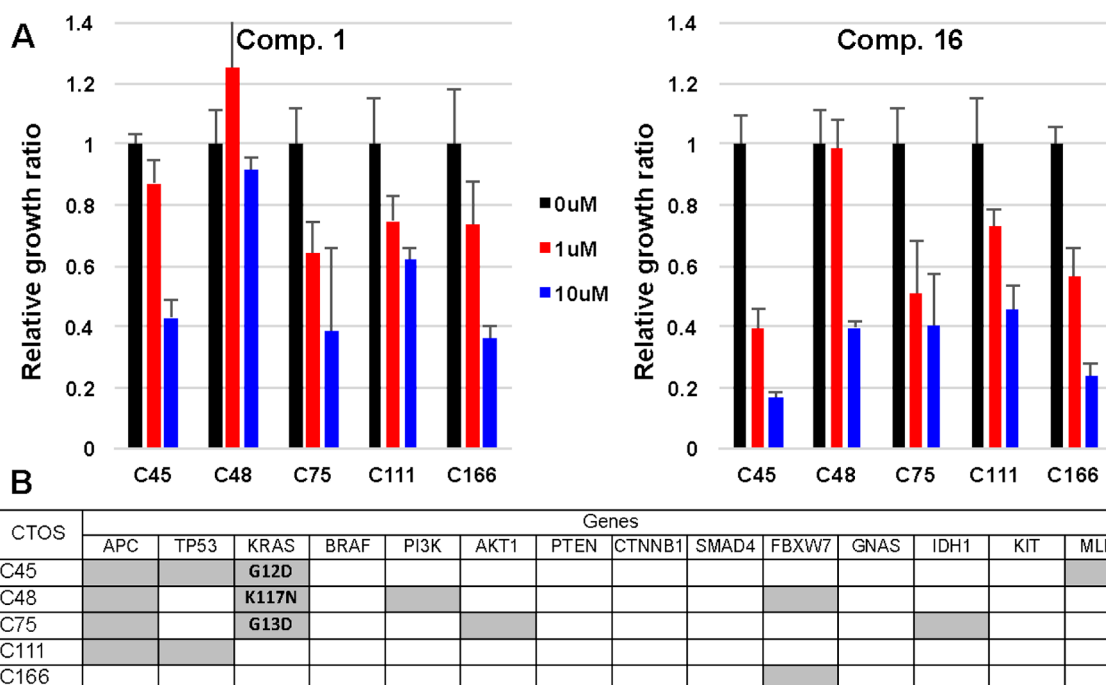
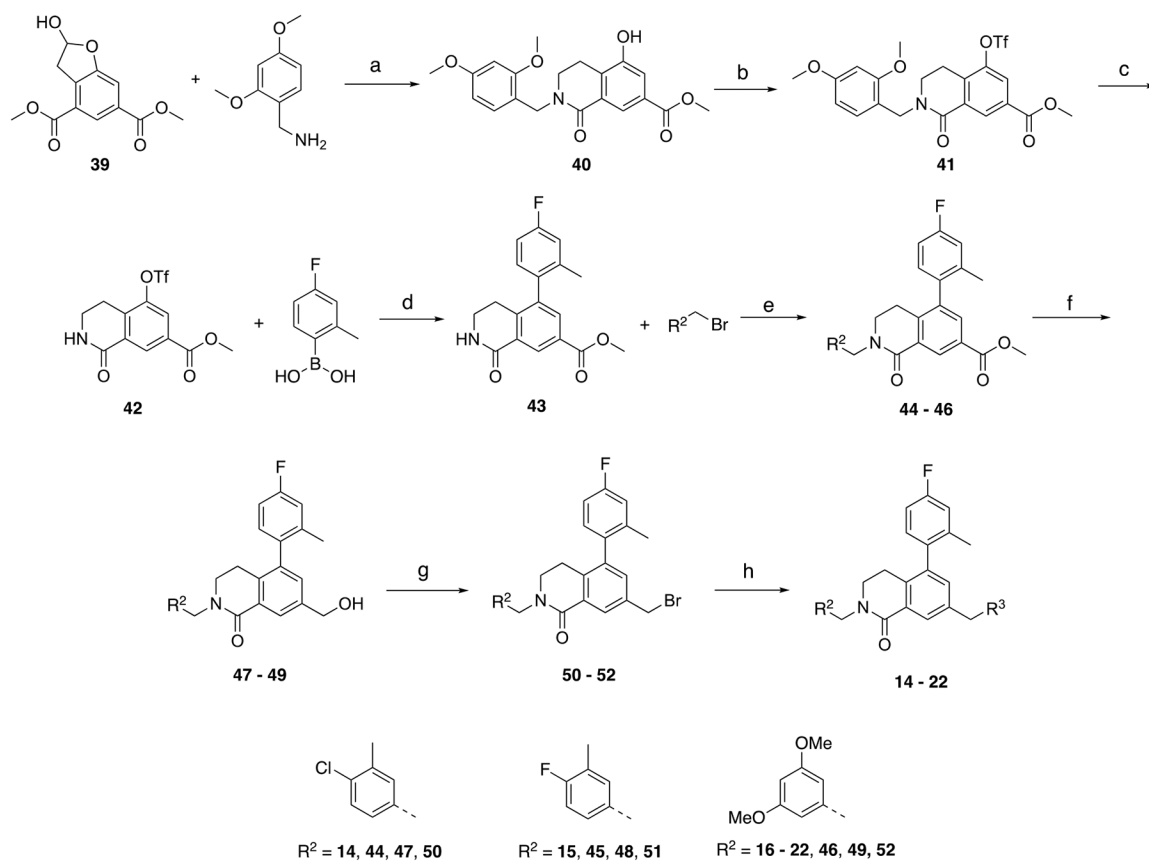


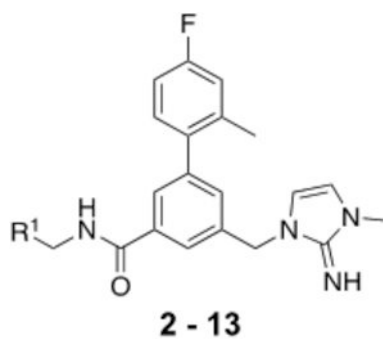
Figure 8. Response of CTOSs to compound **1** and **16**. (A) The sensitivity of CTOSs from five patients dosed with 1 and 10 μM compound **1** and **16**. Relative growth ratios were calculated by comparing with 0.1% DMSO control. (B) Mutation profiles of the CTOSs. Gray block indicated presence of a mutation.

**Scheme 2.****Synthesis of Dihydroisoquinolinone Series Compounds 14 – 22^a**

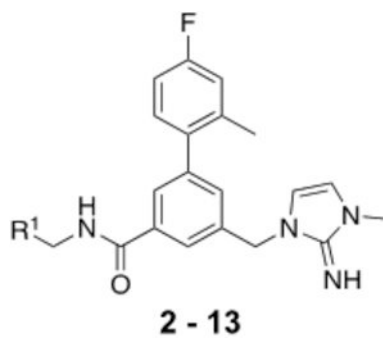
^a R^2 and R^3 are defined in Table 2. Conditions: (a) $\text{NaBH}(\text{OAc})_3$, CH_2Cl_2 , rt, overnight, 65%; (b) phenyl triflimide, $i\text{-Pr}_2\text{NEt}$, CH_2Cl_2 , rt, overnight, 75%; (c) TFA, anisole, CH_2Cl_2 , rt, overnight, 78%; (d) (4-fluoro-2-methylphenyl) boronic acid, $\text{Pd}(\text{PPh}_3)_4$, Na_2CO_3 , 1,4-dioxane: H_2O , 80 °C, overnight, 93%; (e) R^2 -alkyl bromide, NaH, DMF, 0 °C, 2 h, 57% - quant.; (f) LiBHEt_3 , THF, 0 °C, 1 h, 68% - quant.; (g) PBr_3 , CH_2Cl_2 , 0 °C, 4 h, 54 – 93%; (h) R^3 -amine, $i\text{-Pr}_2\text{NEt}$, KI, MeCN, 50 °C, overnight, 35 – 84%.

Table 1.

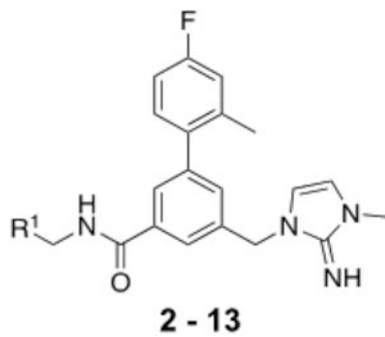
SAR Profile of Substituted Benzamide WDR5 WIN site inhibitors



compnd	R ¹ =	K _d (nM)	HMT IC ₅₀ (nM)		Cell Proliferation Assays GI ₅₀ (nM)			Selectivity
		TR-FRET	WDR5	MLL1	MV4:11	Molml3	K562	
2		1.5 ±0.80	43.3	2300 ± 620	2000 ± 230	13000 ± 3000	5	
3		0.50 ±0.010	55.0	2400 ± 660	2700 ± 440	18000 ±6300	7	
4		0.14 ±0.065	14.0	870 ± 320	840 ± 93	6400 ±1400	7	
5		0.16 ±0.026	9.9	820 ± 400	970 ± 400	15000 ±850	18	



compnd	R ¹ =	K _d (nM) TR- FRET	HMT IC ₅₀ (nM)		Cell Proliferation Assays GI ₅₀ (nM)			Selectivity
			WDR5	MLL1	MV4:11	Molml3	K562	
6		16 ± 14	>3000	13000±1300	7600 ± 460	28000 ± 2400	2	
7		0.030 ±0.014	3.4	390 ±150	390 ± 52	3600 ±1100	9	
8		0.090 ± 0.002	28.4	1300±190	1500 ±220	10000 ± 3400	8	
9		0.032 ± 0.005	11.6	360 ± 200	405 ± 83	7600±1500	21	
10		0.035 ± 0.002	8.6	240 ± 28	300 ± 49	12000 ± 3800	50	



compnd	R ¹ =	K _d (nM) TR- FRET	HMT IC ₅₀ (nM)		Cell Proliferation Assays GI ₅₀ (nM)			Selectivity K562/ MV4:11
			WDR5	MLL1	MV4:11	Molml3	K562	
11		0.055 ± 0.021	23.9		340 ± 86	510 ± 140	5900 ± 1200	17
12		0.061 ± 0.023	3.4		490 ± 25	580 ± 170	4900 ± 940	10
13		0.049 ± 0.008	3.4		470 ± 25	480 ± 110	15000 ± 3600	32

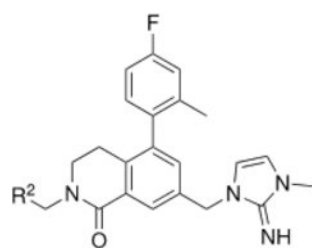
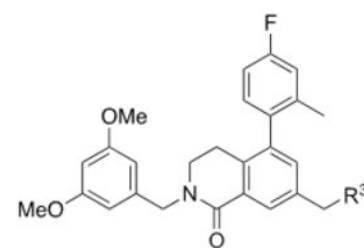
^aTR-FRET K_i , and cell proliferation GI₅₀ values represent four independent replicate determinations ± the standard deviation.

^bHistone methyltransferase inhibition (HMT) IC₅₀ values represent two independent replicate determinations.

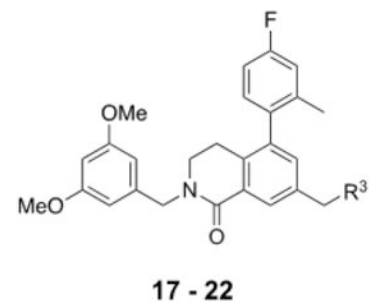
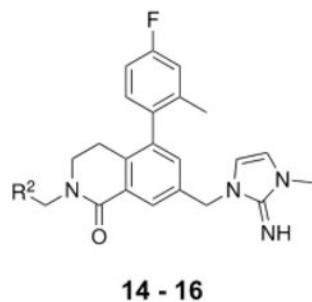
^cSelectivity is defined as GI₅₀, K562/GI₅₀, MV4:11.

Table 2.

Biochemical and Cellular Activity of Compounds Containing Dihydroisoquinolinone Core

**14 - 16****17 - 22**

compnd	R ² =	K _d (nM) TR-FRET	HMT IC ₅₀ (nM)		Cell Proliferation Assays GI ₅₀ (nM)			Selectivity K562/ MV4:11
			WDR5	MLL1	MV4:11	Molml3	K562	
14		0.027 ± 0.008	4.7	240 ± 120	340 ± 68	8800 ± 1300	37	
15		<0.02	<2.0	44 ± 25	55 ± 11	5400 ± 1700	120	
16		<0.02	2.2	38 ± 9.0	78 ± 13	8000 ± 4100	210	
R ³ =								
17		0.043 ± 0.019	2.5	110 ± 37	200 ± 69	8600 ± 1300	78	
18		0.030 ± 0.018	2.3	150 ± 43	240 ± 7.1	3700 ± 1000	25	



compnd	R ² =	K _d (nM) TR-FRET		Cell Proliferation Assays GI ₅₀ (nM)			Selectivity K562/ MV4:11
		WDR5	MLL1	MV4:11	Molml3	K562	
19		<0.02	4.0	180 ± 56	330 ± 61	3400 ± 930	19
20		0.033 ± 0.009	15	290 ± 36	570 ± 39	2800 ± 490	10
21		0.063 ± 0.020	14	400 ± 89	730 ± 100	4900 ± 1200	12
22		0.023 ± 0.010	<2.0	84 ± 10	180 ± 33	2900 ± 190	35

^aTR-FRET K_d, and cell proliferation GI₅₀ values represent four independent replicate determinations ± the standard deviation.

^bHistone methyltransferase inhibition (HMT) IC₅₀ values represent two independent replicate determinations.

^cSelectivity is defined as GI₅₀, K562/GI₅₀, MV4:11.

Table 3.

Anti-proliferative Activity of Compound 16 in MYC-driven Cancers.

Compnd	Cell line GI ₅₀ (μM) ^a					
	CHP-134	Ramos	Raji	Daudi	SW620	SW480
1	2.7 ± 0.8	7.1 ± 1.4	16 ± 2.2	6.8 ± 4.0	6.5 ± 3.4	>29
16	0.26 ± 0.08	0.49 ± 0.24	1.2 ± 0.1	0.58 ± 0.26	3.2 ± 1.2	>22

^aCell proliferation GI₅₀ values represent average of three to five independent replicate determinations ± the standard deviation.

Author Manuscript

Author Manuscript

Author Manuscript

Author Manuscript